Journal of Scientific Computing (2023) 97:48
https://doi.org/10.1007/s10915-023-02365-5

Some Optimally Convergent Algorithms for Decoupling the Computation of Biot's Model

Mingchao Cai[1] · **Huipeng Gu**[2] · **Jingzhi Li**[3] · **Mo Mu**[4]

Received: 31 January 2023 / Revised: 17 September 2023 / Accepted: 20 September 2023

Abstract
We study numerical algorithms for solving Biot's model. Based on a three-field reformulation, we present some algorithms that are inspired by the work of Chaabane et al. (Comput Math Appl 75(7):2328–2337) and Lee (Unconditionally stable second order convergent partitioned methods for multiple-network poroelasticity arXiv:1901.06078, 2019) for decoupling the computation of Biot's model. A new theoretical framework is developed to analyze the algorithms. Considering a uniform temporal discretization, these algorithms solve the coupled model on the first time level. On the remaining time levels, one algorithm solves a reaction-diffusion subproblem first and then solves a generalized Stokes subproblem. Another algorithm reverses the order of solving the two subproblems. Our algorithms manage to decouple the numerical computation of the coupled system while retaining the convergence properties of the original coupled algorithm. Theoretical analysis is conducted to show that these algorithms are unconditionally stable and optimally convergent. Numerical experiments are also carried out to validate the theoretical analysis and demonstrate the advantages of the proposed algorithms.

Keywords Biot's model · Decoupled algorithms · Finite element method · Unconditionally stable

Mathematics Subject Classification 65M60 · 65N30 · 74F10

1 Introduction

The theory of poroelasticity describes the interaction between deformable porous media solids and fluid flow. The fundamental model of poroelasticity is called Biot's model [5, 6], which is a coupled system of partial differential equations (PDEs). It has drawn much attention because of its wide applications in petroleum engineering, geoscience, and biomedical engineering [20]. However, Biot's model is a multiphysics problem involving both elasticity and porous media flow, which leads to numerical difficulties, such as elasticity locking and

✉ Mingchao Cai
cmchao2005@gmail.com

Published online: 07 October 2023

pressure oscillation, particularly for the two-field formulation based model [13, 23, 31, 33]. To overcome these difficulties, discontinuous Galerkin method [29], stabilized Finite Element methods [31, 32], and various three-field or four-field reformulations have been proposed [15, 23, 27, 34]. Following [23, 27], an intermediate variable, called "total pressure", is introduced to develop a three-field formulation for Biot's model in this paper, which allows one to view Biot's model as a combination of a generalized Stokes problem and a reaction-diffusion problem. This reformulation has advantages in several aspects. First, one can apply the classical inf-sup stable Stokes elements for the displacement and the total pressure, and the Lagrange elements for the fluid pressure. Secondly, existing fast solvers in multigrid and domain decomposition methods can be directly invoked. Investigations based on this three-field reformulation may be found in [17, 18, 20, 22–24, 27]. Other relevant works include the optimal order error estimates of a coupled scheme [30] and a virtual element discretization [10].

The numerical difficulties in solving Biot's system call for the development of effective and efficient numerical algorithms. The numerical methods for solving Biot's model can be categorized into three types: (i) The fully-coupled algorithms, in which all variables are solved in a coupled way on each time level [18, 23, 27, 30]; (ii) The iterative algorithms [17, 21, 25], in which submodels are solved iteratively on each time level, using the approximate solution of the previous iteration step until the error tolerance is reached; (iii) The decoupled algorithms [15, 20], in which submodels are solved on each time level yet without iterations. Theoretically, fully-coupled algorithms achieve optimality in stability, convergence, and accuracy, however, are more computationally demanding. Investigation on efficient preconditioners to accelerate the convergence of the Krylov subspace methods can be found in [1, 11, 13, 23]. The preconditioners are applied to various iterative algorithms [7, 16, 17, 21, 25, 34] to reduce the computational cost due to smaller cost for submodels in each iteration, and legacy code can be invoked for each submodel. Among these iterative algorithms, the fixed-stress splitting method is widely used in the engineering community due to its unconditional stability [7, 14, 25]. However, it is important to note that this method may require a certain stabilization parameter to be sufficiently large in order to ensure convergence. Instead of using an iterative procedure, the decoupled algorithms split the original coupled problem into smaller sub-systems to reduce the computational cost. By applying a stabilization parameter, a splitting-based method is devised for the two-field formulation in [14]. To avoid stabilization parameters, several conditionally convergent decoupled algorithms are proposed in [3, 15]. However, most of these existing decoupled approaches assume additional conditions such as the specific storage coefficient $c_0 > 0$ [25], or the weak coupling condition [3], or large enough stabilization parameters in discretization [7, 14, 21, 25, 29].

In this paper, we present some algorithms, which solve a coupled system only on the first time level, while applying decoupled computation on the subsequent time levels. These algorithms are inspired by [14] which is based on a stabilized two-field formulation, and [22], which uses a three-field formulation and considers 2nd-order time schemes for a more general multiple-network Biot's model. Our algorithms can be thought of as a degenerate 1st-order scheme of [22] for the single-network Biot's model. We developed a new theoretical framework to analyze the proposed algorithms. Solving a coupled system on the first time level initially enables us to get the computation started, and retain the approximation accuracy, yet not to impose small time step constraints for stability in time marching for subsequent time levels, (see [15] for the analysis of the stability constraint). Combined with this initialization technique, we may then follow the decoupled algorithms proposed in recent works [20, 22]. We will prove that the algorithms are unconditionally stable and optimally convergent. Since

these new algorithms are decoupled from the second time level, they are not only stable and convergent but also computationally efficient.

The rest of the paper is organized as follows. In Sect. 2, we describe the three-field formulation of Biot's consolidation model and its corresponding variational formulation. The new algorithms are presented in Sect. 3. The convergence analysis of the new algorithms is given in Sect. 4. Finally, in Sect. 5, numerical experiments are given to validate the theoretical results.

2 Mathematical Formulations

Let $\Omega \subset \mathbb{R}^d$ ($d = 2$ or 3) be a bounded polygonal domain with boundary $\partial\Omega$. We consider the quasi-static Biot system which reads as follows.

$$-\mathrm{div}\sigma(\boldsymbol{u}) + \alpha\nabla p = \boldsymbol{f}, \tag{1}$$

$$\partial_t(c_0 p + \alpha \mathrm{div}\boldsymbol{u}) - \mathrm{div}K(\nabla p - \rho_f \boldsymbol{g}) = Q_s, \tag{2}$$

where

$$\sigma(\boldsymbol{u}) = 2\mu\varepsilon(\boldsymbol{u}) + \lambda(\mathrm{div}\boldsymbol{u})\boldsymbol{I}, \quad \varepsilon(\boldsymbol{u}) = \frac{1}{2}\left[\nabla\boldsymbol{u} + (\nabla\boldsymbol{u})^T\right].$$

In these equations, the primary unknowns are the displacement vector of the solid $\boldsymbol{u}$ and the fluid pressure p, the coefficient $\alpha > 0$ is the Biot–Willis constant which is close to 1, $\boldsymbol{f}$ is the body force, $c_0 \geq 0$ is the specific storage coefficient, K represents the hydraulic conductivity, ρ_f is the fluid density, $\boldsymbol{g}$ is the gravitational acceleration, Q_s is a source or sink term, $\boldsymbol{I}$ represents the identity matrix, the Lamé constants λ and μ are related to Young's modulus E and the Poisson ratio ν as follows (Fig. 1):

$$\lambda = \frac{E\nu}{(1+\nu)(1-2\nu)}, \quad \mu = \frac{E}{2(1+\nu)}.$$

Suitable boundaries and initial conditions should be provided to complete the system. As shown in Fig. 1, we assume $\partial\Omega = \Gamma_{\boldsymbol{u}} \cup \Gamma_\sigma = \Gamma_p \cup \Gamma_q$ with $|\Gamma_{\boldsymbol{u}}| > 0, |\Gamma_p| > 0$, and consider the following boundary conditions:

$$\boldsymbol{u} = \boldsymbol{0} \quad \text{on } \Gamma_{\boldsymbol{u}}, \tag{3}$$

$$(\sigma(\boldsymbol{u}) - \alpha p\boldsymbol{I})\boldsymbol{n} = \boldsymbol{h} \quad \text{on } \Gamma_\sigma, \tag{4}$$

$$p = 0 \quad \text{on } \Gamma_p, \tag{5}$$

$$K(\nabla p - \rho_f \boldsymbol{g}) \cdot \boldsymbol{n} = g_2 \quad \text{on } \Gamma_q, \tag{6}$$

where $\boldsymbol{n}$ is the unit outward normal to the boundary. The initial conditions are given by

$$\boldsymbol{u}(0) = \boldsymbol{u}^0, \quad p(0) = p^0. \tag{7}$$

Following [23, 27], we introduce an intermediate variable ξ, called "total pressure", defined by $\xi = \alpha p - \lambda \mathrm{div}\boldsymbol{u}$. Then, (1)–(2) can be rewritten as the following three-field formulation.

$$-2\mu\mathrm{div}(\varepsilon(\boldsymbol{u})) + \nabla\xi = \boldsymbol{f}, \tag{8}$$

$$\mathrm{div}\boldsymbol{u} + \frac{1}{\lambda}\xi - \frac{\alpha}{\lambda}p = 0, \tag{9}$$

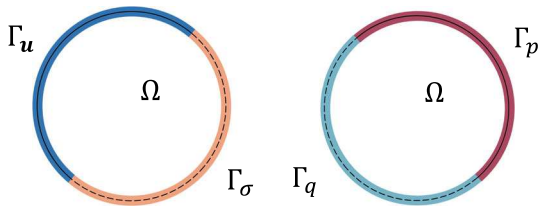

Fig. 1 Two distinct types of boundary conditions can be imposed on $\partial\Omega$: one is for the displacement (left), and the other is for the pressure (right)

$$\left(c_0 + \frac{\alpha^2}{\lambda}\right)\partial_t p - \frac{\alpha}{\lambda}\partial_t \xi - \mathrm{div} K(\nabla p - \rho_f \boldsymbol{g}) = Q_s. \tag{10}$$

After the reformulation, the boundary conditions (3)–(6) and initial conditions (7) with $\xi(0) = \alpha p^0 - \lambda \mathrm{div}\boldsymbol{u}^0$ can still be applied. For ease of presentation, we assume the gravity acceleration $\boldsymbol{g} = \boldsymbol{0}$ in the rest of the paper.

Let $H^k(\Omega)$ be the classical Sobolev spaces with norm $\|\cdot\|_{H^k(\Omega)}$. Denote $H^k_{0,\Gamma}(\Omega)$ be the subspace of $H^k(\Omega)$ with the vanishing trace on $\Gamma \subset \partial\Omega$. In this paper, we will use $(\cdot,\cdot)$ and $\langle\cdot,\cdot\rangle$ to denote the standard $L^2(\Omega)$ and $L^2(\partial\Omega)$ inner products, respectively. Moreover, we use C to denote a generic positive constant independent of mesh sizes and $x \lesssim y$ to denote $x \le Cy$. Let $\boldsymbol{V} = \boldsymbol{H}^1_{0,\Gamma_{\boldsymbol{u}}}(\Omega)$, $W = L^2(\Omega)$ and $M = H^1_{0,\Gamma_p}(\Omega)$. For $\boldsymbol{u}, \boldsymbol{v} \in \boldsymbol{V}$, $\xi, \phi \in W$, and $p, \psi \in M$, we define the following bilinear forms:

$$\begin{aligned}
&a_1(\boldsymbol{u}, \boldsymbol{v}) = 2\mu \int_\Omega \varepsilon(\boldsymbol{u}) : \varepsilon(\boldsymbol{v}), \quad b(\boldsymbol{v}, \phi) = \int_\Omega \phi\, \mathrm{div}\boldsymbol{v},\\
&a_2(\xi, \phi) = \frac{1}{\lambda}\int_\Omega \xi\phi, \qquad\qquad c(p, \phi) = \frac{\alpha}{\lambda}\int_\Omega p\phi,\\
&a_3(p, \psi) = \left(c_0 + \frac{\alpha^2}{\lambda}\right)\int_\Omega p\psi, \quad d(p, \psi) = K\int_\Omega \nabla p \cdot \nabla\psi.
\end{aligned}$$

Multiplying (8)–(10) by test functions, integrating by parts, and applying boundary conditions (3)–(6) yields the following variational formulation: for a given $t > 0$, find $(\boldsymbol{u}, \xi, p) \in \boldsymbol{V} \times W \times M$ such that

$$a_1(\boldsymbol{u}, \boldsymbol{v}) - b(\boldsymbol{v}, \xi) = (\boldsymbol{f}, \boldsymbol{v}) + \langle \boldsymbol{h}, \boldsymbol{v}\rangle_{\Gamma_\sigma}, \qquad \forall \boldsymbol{v} \in \boldsymbol{V}, \tag{11}$$

$$b(\boldsymbol{u}, \phi) + a_2(\xi, \phi) - c(p, \phi) = 0, \qquad \forall \phi \in W, \tag{12}$$

$$a_3(\partial_t p, \psi) - c(\psi, \partial_t \xi) + d(p, \psi) = (Q_s, \psi) + \langle g_2, \psi\rangle_{\Gamma_q}, \qquad \forall \psi \in M. \tag{13}$$

The well-posedness of Problem (11)–(13) is established in [27]. The Korn's inequality [26] holds on $\boldsymbol{V}$, that is, there exists a constant $C_k = C_k(\Omega, \Gamma_{\boldsymbol{u}}) > 0$ such that

$$\|\boldsymbol{v}\|_{H^1(\Omega)} \le C_k \|\varepsilon(\boldsymbol{v})\|_{L^2(\Omega)}, \quad \forall \boldsymbol{v} \in \boldsymbol{V}. \tag{14}$$

Furthermore, the following inf-sup condition [8] holds: there exists a constant $\beta > 0$ depending only on Ω and $\Gamma_{\boldsymbol{u}}$ such that

$$\sup_{\boldsymbol{v}\in\boldsymbol{V}} \frac{b(\boldsymbol{v}, \phi)}{\|\boldsymbol{v}\|_{H^1(\Omega)}} \ge \beta \|\phi\|_{L^2(\Omega)}, \quad \forall \phi \in W.$$

3 Finite Element Discretization and Numerical Algorithms

Let $\mathcal{T}_h$ be a partition of the domain Ω into triangles in $\mathbb{R}^2$ or tetrahedrons in $\mathbb{R}^3$, and h be the maximum diameter over all elements in the mesh. We define finite element spaces on $\mathcal{T}_h$

$$\begin{aligned}
\boldsymbol{V}_h &:= \{\boldsymbol{v}_h \in \boldsymbol{H}^1_{0,\Gamma_{\boldsymbol{u}}}(\Omega) \cap \boldsymbol{C}^0(\bar{\Omega});\ \boldsymbol{v}_h|_E \in \boldsymbol{P}_k(E), \quad \forall E \in \mathcal{T}_h\},\\
W_h &:= \{\phi_h \in L^2(\Omega) \cap C^0(\bar{\Omega});\ \phi_h|_E \in P_{k-1}(E), \quad \forall E \in \mathcal{T}_h\},\\
M_h &:= \{\psi_h \in H^1_{0,\Gamma_p}(\Omega) \cap C^0(\bar{\Omega});\ \psi_h|_E \in P_l(E), \quad \forall E \in \mathcal{T}_h\},
\end{aligned}$$

where $k \geq 2$ and $l \geq 1$ are integers. In this paper, the Taylor-Hood elements are adopted for the pair $(\boldsymbol{u}, \xi)$, and the Lagrange finite elements are adopted for p, respectively. As we use a stable Stokes element pair, the corresponding finite element spaces satisfy the following discrete inf-sup condition, i.e., there exists a positive constant $\tilde{\beta}$ independent of h such that

$$\sup_{\boldsymbol{v}_h \in \boldsymbol{V}_h} \frac{b(\boldsymbol{v}_h, \phi_h)}{\|\boldsymbol{v}_h\|_{H^1(\Omega)}} \geq \tilde{\beta}\|\phi_h\|_{L^2(\Omega)}, \quad \forall \phi_h \in W_h. \tag{15}$$

Following the common practice as in [24, 30], two projection operators are introduced. First, the Stokes projection operator $\boldsymbol{R}_{\boldsymbol{u}} \times R_\xi : \boldsymbol{V} \times W \to \boldsymbol{V}_h \times W_h$ is defined by

$$a_1(\boldsymbol{R}_{\boldsymbol{u}}\boldsymbol{u}, \boldsymbol{v}_h) - b(\boldsymbol{v}_h, R_\xi \xi) = a_1(\boldsymbol{u}, \boldsymbol{v}_h) - b(\boldsymbol{v}_h, \xi), \quad \forall \boldsymbol{v}_h \in \boldsymbol{V}_h, \tag{16}$$

$$b(\boldsymbol{R}_{\boldsymbol{u}}\boldsymbol{u}, \phi_h) = b(\boldsymbol{u}, \phi_h), \quad \forall \phi_h \in W_h. \tag{17}$$

Second, the elliptic projection operator $R_p : M \to M_h$ is defined by

$$d(R_p p, \psi_h) = d(p, \psi_h), \quad \forall \psi_h \in M_h. \tag{18}$$

If $\boldsymbol{u} \in \boldsymbol{H}^{k+1}_{0,\Gamma_{\boldsymbol{u}}}(\Omega)$, $\xi \in H^k(\Omega)$, and $p \in H^{l+1}_{0,\Gamma_p}(\Omega)$, then the following error estimates hold for the Stokes projection operator and the elliptic projection operator [9].

$$\|\boldsymbol{u} - \boldsymbol{R}_{\boldsymbol{u}}\boldsymbol{u}\|_{H^1(\Omega)} + \|\xi - R_\xi \xi\|_{L^2(\Omega)} \leq Ch^k(\|\boldsymbol{u}\|_{H^{k+1}(\Omega)} + \|\xi\|_{H^k(\Omega)}), \tag{19}$$

$$\|p - R_p p\|_{H^1(\Omega)} \leq Ch^l \|p\|_{H^{l+1}(\Omega)}. \tag{20}$$

Under the assumption that the domain Ω has the full elliptic regularity [24], there holds

$$\|p - R_p p\|_{L^2(\Omega)} \leq Ch^{l+1} \|p\|_{H^{l+1}(\Omega)}. \tag{21}$$

An equidistant partition $0 = t_0 < t_1 < \cdots < t_{N+1} = T$ with a step size $\Delta t = \frac{T}{N+1}$ is used for the time discretization. Denote $\boldsymbol{u}^n = \boldsymbol{u}(t_n)$, $\xi^n = \xi(t_n)$ and $p^n = p(t_n)$. The initial conditions may then be approximated by $\boldsymbol{u}_h^0 = \boldsymbol{R}_{\boldsymbol{u}}\boldsymbol{u}^0$, $\xi_h^0 = R_\xi \xi^0 = R_\xi(\alpha p^0 - \lambda \mathrm{div}\boldsymbol{u}^0)$, and $p_h^0 = R_p p^0$ in terms of the projection operators and the initial data in (7) from the original model.

Based on the three-field formulation (8)–(10), the backward Euler method for the time discretization leads to a coupled scheme.

Coupled algorithm: Given $(\boldsymbol{u}_h^n, \xi_h^n, p_h^n) \in \boldsymbol{V}_h \times W_h \times M_h$, find $(\boldsymbol{u}_h^{n+1}, \xi_h^{n+1}, p_h^{n+1}) \in \boldsymbol{V}_h \times W_h \times M_h$ such that

$$a_1(\boldsymbol{u}_h^{n+1}, \boldsymbol{v}_h) - b(\boldsymbol{v}_h, \xi_h^{n+1}) = (\boldsymbol{f}^{n+1}, \boldsymbol{v}_h) + \langle \boldsymbol{h}^{n+1}, \boldsymbol{v}_h \rangle_{\Gamma_\sigma}, \quad \forall \boldsymbol{v}_h \in \boldsymbol{V}_h, \tag{22}$$

$$b(\boldsymbol{u}_h^{n+1}, \phi_h) + a_2(\xi_h^{n+1}, \phi_h) - c(p_h^{n+1}, \phi_h) = 0, \quad \forall \phi_h \in W_h, \tag{23}$$

$$a_3\left(\frac{p_h^{n+1} - p_h^n}{\Delta t}, \psi_h\right) - c\left(\psi_h, \frac{\xi_h^{n+1} - \xi_h^n}{\Delta t}\right)$$

$$+ d(p_h^{n+1}, \psi_h) = (Q_s^{n+1}, \psi_h) + \langle g_2^{n+1}, \psi_h \rangle_{\Gamma_q}, \qquad \forall \psi_h \in M_h. \tag{24}$$

The **Coupled algorithm** is unconditionally stable and convergent. To decouple the computation involving three governing variables on the current time level in the coupled system, we note that from past experiences, simply approximating any variable on the current time level $n+1$ in (22) and (23) by their computed data from the previous time level would easily lead to certain explicit behavior and thus destroy the stability property in the implicit coupled algorithm. For example, the authors of [3] have highlighted the essential requirement for imposing additional conditions on the physical parameters in such scenarios. Mathematically, the major difficulty lies in that the continuous equations (11) and (12) corresponding to (22) and (23) are time-independent, only describing certain physical balance conditions in space. To enable the information of the governing variables, essentially the displacement and pressure, to be carried on in computation as time evolves, we may instead mathematically equivalently first take the time derivative on (12) to replace it by

$$b(\partial_t \boldsymbol{u}, \phi) + a_2(\partial_t \xi, \phi) - c(\partial_t p, \phi) = 0, \qquad \forall \phi \in W,$$

and then apply the implicit backward Euler scheme for time discretization to obtain the discrete counterpart to replace (23) by

$$b\left(\frac{\boldsymbol{u}_h^{n+1} - \boldsymbol{u}_h^n}{\Delta t}, \phi_h\right) + a_2\left(\frac{\xi_h^{n+1} - \xi_h^n}{\Delta t}, \phi_h\right) - c\left(\frac{p_h^{n+1} - p_h^n}{\Delta t}, \phi_h\right) = 0, \qquad \forall \phi_h \in W_h.$$

This leads to a new coupled algorithm, which is also an implicit scheme and thus is unconditionally stable and convergent, too. However, it now allows the displacement and pressure data, as well as their physical balance condition in space, to be carried on as time evolves. Moreover, the decoupling may be realized by further approximating the time derivative finite difference term $\frac{p_h^{n+1} - p_h^n}{\Delta t}$ with the computed data on the previous time level $\frac{p_h^n - p_h^{n-1}}{\Delta t}$ for decoupling the pressure from the displacement, yet the stability of the displacement is still enforced by its implicit in-time discretization for its dynamics. This strategy has also been applied in the literature, such as similar to [14, 20, 22], and in decoupling fluid-solid interactions computation where intrinsic Robin condition based decoupled algorithms are devised [12, 35]. However, this is a two-step procedure and requires computed data for pressure $\frac{p_h^n - p_h^{n-1}}{\Delta t}$ on the previous two time levels. To start with the decoupled computation on subsequent time levels, we propose to first apply the above coupled, yet one-step, algorithm to compute $(\boldsymbol{u}_h^1, \xi_h^1, p_h^1)$ on the first time level, followed on subsequent time levels by alternatively solving the generalized Stokes equations and the reaction-diffusion problem independently. This results in the first version of the decoupled algorithms referred to as the **StR algorithm**.

StR algorithm:

Initial step: Given $(\boldsymbol{u}_h^0, \xi_h^0, p_h^0) \in \boldsymbol{V}_h \times W_h \times M_h$, find $(\boldsymbol{u}_h^1, \xi_h^1, p_h^1) \in \boldsymbol{V}_h \times W_h \times M_h$ such that

$$a_1(\boldsymbol{u}_h^1, \boldsymbol{v}_h) - b(\boldsymbol{v}_h, \xi_h^1) = (\boldsymbol{f}^1, \boldsymbol{v}_h) + \langle \boldsymbol{h}^1, \boldsymbol{v}_h \rangle_{\Gamma_\sigma}, \qquad \forall \boldsymbol{v}_h \in \boldsymbol{V}_h, \tag{25}$$

$$b(\boldsymbol{u}_h^1, \phi_h) + a_2(\xi_h^1, \phi_h) - c(p_h^1, \phi_h) = 0, \qquad \forall \phi_h \in W_h, \tag{26}$$

$$a_3\left(\frac{p_h^1 - p_h^0}{\Delta t}, \psi_h\right) - c\left(\psi_h, \frac{\xi_h^1 - \xi_h^0}{\Delta t}\right)$$

$$+ d(p_h^1, \psi_h) = (Q_s^1, \psi_h) + \langle g_2^1, \psi_h \rangle_{\Gamma_q}, \qquad \forall \psi_h \in M_h. \tag{27}$$

Subsequent steps: For $n \geq 1$,
StR step 1: given $p_h^{n-1}, p_h^n \in M_h$, find $(\boldsymbol{u}_h^{n+1}, \xi_h^{n+1}) \in \boldsymbol{V}_h \times W_h$ such that

$$a_1(\boldsymbol{u}_h^{n+1}, \boldsymbol{v}_h) - b(\boldsymbol{v}_h, \xi_h^{n+1}) = (\boldsymbol{f}^{n+1}, \boldsymbol{v}_h) + \langle \boldsymbol{h}^{n+1}, \boldsymbol{v}_h \rangle_{\Gamma_\sigma}, \qquad \forall \boldsymbol{v}_h \in \boldsymbol{V}_h, \tag{28}$$

$$b(\boldsymbol{u}_h^{n+1} - \boldsymbol{u}_h^n, \phi_h) + a_2(\xi_h^{n+1} - \xi_h^n, \phi_h) = c(p_h^n - p_h^{n-1}, \phi_h), \quad \forall \phi_h \in W_h. \tag{29}$$

StR step 2: find $p_h^{n+1} \in M_h$ such that

$$a_3\left(\frac{p_h^{n+1} - p_h^n}{\Delta t}, \psi_h\right) - c\left(\psi_h, \frac{\xi_h^{n+1} - \xi_h^n}{\Delta t}\right) + d(p_h^{n+1}, \psi_h) = (Q_s^{n+1}, \psi_h) + \langle g_2^{n+1}, \psi_h \rangle_{\Gamma_q}, \qquad \forall \psi_h \in M_h. \tag{30}$$

Alternatively, one can solve the reaction-diffusion problem first and then the generalized Stokes equations by decoupling ξ from p in (24) through the approximation of the backward difference of ξ using the computed data on the previous time levels similarly, which is referred to as the **RtS algorithm**.
RtS algorithm:
Initial step: The same as (25) – (27)
Subsequent steps: For $n \geq 1$,
RtS step 1: given $\xi_h^{n-1}, \xi_h^n \in W_h$, find $p_h^{n+1} \in M_h$ such that

$$a_3\left(\frac{p_h^{n+1} - p_h^n}{\Delta t}, \psi_h\right) + d(p_h^{n+1}, \psi_h) = (Q_s^{n+1}, \psi_h) + \langle g_2^{n+1}, \psi_h \rangle_{\Gamma_q} + c\left(\psi_h, \frac{\xi_h^n - \xi_h^{n-1}}{\Delta t}\right), \qquad \forall \psi_h \in M_h. \tag{31}$$

RtS step 2: find $(\boldsymbol{u}_h^{n+1}, \xi_h^{n+1}) \in \boldsymbol{V}_h \times W_h$ such that

$$a_1(\boldsymbol{u}_h^{n+1}, \boldsymbol{v}_h) - b(\boldsymbol{v}_h, \xi_h^{n+1}) = (\boldsymbol{f}^{n+1}, \boldsymbol{v}_h) + \langle \boldsymbol{h}^{n+1}, \boldsymbol{v}_h \rangle_{\Gamma_\sigma}, \qquad \forall \boldsymbol{v}_h \in \boldsymbol{V}_h, \tag{32}$$

$$b(\boldsymbol{u}_h^{n+1} - \boldsymbol{u}_h^n, \phi_h) + a_2(\xi_h^{n+1} - \xi_h^n, \phi_h) - c(p_h^{n+1} - p_h^n, \phi_h) = 0, \quad \forall \phi_h \in W_h. \tag{33}$$

4 Convergence Analysis

We now present the convergence analysis and error estimates for the decoupled **StR algorithm** and **RtS algorithm**, where the following regularity assumptions are imposed.

Assumption 1 Assume that $\boldsymbol{u} \in L^\infty(0, T; \boldsymbol{H}_{0,\Gamma_{\boldsymbol{u}}}^{k+1}(\Omega))$, $\partial_t \boldsymbol{u} \in L^2(0, T; \boldsymbol{H}_{0,\Gamma_{\boldsymbol{u}}}^{k+1}(\Omega))$, $\partial_{tt} \boldsymbol{u} \in L^2(0, T; \boldsymbol{H}_{0,\Gamma_{\boldsymbol{u}}}^{1}(\Omega))$, $\xi \in L^\infty(0, T; H^k(\Omega))$, $\partial_t \xi \in L^2(0, T; H^k(\Omega))$, $\partial_{tt} \xi \in L^2(0, T; L^2(\Omega))$, $p \in L^\infty(0, T; H_{0,\Gamma_p}^{l+1}(\Omega))$, $\partial_t p \in L^2(0, T; H_{0,\Gamma_p}^{l+1}(\Omega))$, $\partial_{tt} p \in L^2(0, T; L^2(\Omega))$.

For ease of presentation, the error terms are decomposed as

$$e_{\boldsymbol{u}}^n = \boldsymbol{u}^n - \boldsymbol{u}_h^n = (\boldsymbol{u}^n - \boldsymbol{R}_{\boldsymbol{u}} \boldsymbol{u}^n) + (\boldsymbol{R}_{\boldsymbol{u}} \boldsymbol{u}^n - \boldsymbol{u}_h^n) =: e_{\boldsymbol{u}}^{I,n} + e_{\boldsymbol{u}}^{h,n},$$

$$e_\xi^n = \xi^n - \xi_h^n = (\xi^n - R_\xi \xi^n) + (R_\xi \xi^n - \xi_h^n) =: e_\xi^{I,n} + e_\xi^{h,n},$$

$$e_p^n = p^n - p_h^n = (p^n - R_p p^n) + (R_p p^n - p_h^n) =: e_p^{I,n} + e_p^{h,n}.$$

We also denote

$$D_{\boldsymbol{u}}^{n+1} := e_{\boldsymbol{u}}^{h,n+1} - e_{\boldsymbol{u}}^{h,n}, \quad D_\xi^{n+1} := e_\xi^{h,n+1} - e_\xi^{h,n}, \quad D_p^{n+1} := e_p^{h,n+1} - e_p^{h,n}.$$

Both the **StR algorithm** and **RtS algorithm** involve the **Initial step** (25)–(27), which has the following error estimates for $(\boldsymbol{u}_h^1, \xi_h^1, p_h^1)$. The proof is a direct consequence of Theorem 4.1 and Theorem 4.2 for the **Coupled algorithm** in [18].

Theorem 1 *Let $(\boldsymbol{u}, \xi, p)$ and $(\boldsymbol{u}_h^1, \xi_h^1, p_h^1)$ be solutions of Eqs. (11)–(13) and Eqs. (25)–(27), respectively. Under **Assumption 1**, we have*

$$\begin{aligned}
&\frac{1}{\Delta t}\left(\|\varepsilon(D_{\boldsymbol{u}}^1)\|_{L^2(\Omega)}^2 + \|D_\xi^1\|_{L^2(\Omega)}^2 + \|D_p^1\|_{L^2(\Omega)}^2\right) + \|\nabla e_p^{h,1}\|_{L^2(\Omega)}^2 \\
&\lesssim (\Delta t)^2 \int_0^{t_1} \left(\|\partial_{tt}\boldsymbol{u}\|_{H^1(\Omega)}^2 + \|\partial_{tt}\xi\|_{L^2(\Omega)}^2 + \|\partial_{tt}p\|_{L^2(\Omega)}^2\right) ds \\
&+ h^{2k} \int_0^{t_1} \left(\|\partial_t \boldsymbol{u}\|_{H^{k+1}(\Omega)}^2 + \|\partial_t \xi\|_{H^k(\Omega)}^2\right) ds + h^{2l+2} \int_0^{t_1} \|\partial_t p\|_{H^{l+1}(\Omega)}^2 ds, \qquad (34)
\end{aligned}$$

and

$$\begin{aligned}
&\|\varepsilon(e_{\boldsymbol{u}}^{h,1})\|_{L^2(\Omega)}^2 + \|e_\xi^{h,1}\|_{L^2(\Omega)}^2 + \|e_p^{h,1}\|_{L^2(\Omega)}^2 \\
&\lesssim (\Delta t)^2 \int_0^{t_1} \left(\|\partial_{tt}\boldsymbol{u}\|_{H^1(\Omega)}^2 + \|\partial_{tt}\xi\|_{L^2(\Omega)}^2 + \|\partial_{tt}p\|_{L^2(\Omega)}^2\right) ds \\
&+ h^{2k} \int_0^{t_1} \left(\|\partial_t \boldsymbol{u}\|_{H^{k+1}(\Omega)}^2 + \|\partial_t \xi\|_{H^k(\Omega)}^2\right) ds + h^{2l+2} \int_0^{t_1} \|\partial_t p\|_{H^{l+1}(\Omega)}^2 ds. \qquad (35)
\end{aligned}$$

We also cite below two propositions that are used frequently in our following analysis, their proofs can also be found in [18].

Proposition 1 *Let $f : \mathbb{R} \to \mathbb{R}$ be a function that has $k+1$ continuous derivatives on an open interval (a, b). For any $t_0, t \in (a, b)$, there holds*

$$f(t) = f(t_0) + f'(t_0)(t - t_0) + \cdots + \frac{f^{(k)}(t_0)}{k!}(t - t_0)^k + \frac{1}{k!}\int_{t_0}^t f^{(k+1)}(s)(t - s)^k ds.$$

Then, the following estimate for the L^2-norm of the last term holds.

$$\left\| \frac{1}{k!}\int_{t_0}^t f^{(k+1)}(s)(t - s)^k ds \right\|_{L^2(\Omega)}^2 \lesssim (b - a)^{2k+1} \left| \int_{t_0}^t \|f^{(k+1)}\|_{L^2(\Omega)}^2 ds \right|. \qquad (36)$$

Proposition 2 *Let B be a symmetric bilinear form, there holds*

$$2B(u, u - v) = B(u, u) - B(v, v) + B(u - v, u - v),$$

which immediately implies the following inequality

$$2B(u, u - v) \geq B(u, u) - B(v, v). \qquad (37)$$

4.1 A Priori Error Estimates for the StR Algorithm

In this subsection, we present the a priori error estimates of the **StR algorithm**.

Theorem 2 *Let* $(\boldsymbol{u}, \xi, p)$ *and* $(\boldsymbol{u}_h^{n+1}, \xi_h^{n+1}, p_h^{n+1})$ *for* $n \geq 1$ *be the solutions of Eqs.* (11)–(13) *and Eqs.* (28)–(30)*, respectively. Under* ***Assumption*** 1*, there holds*

$$\begin{aligned}
&\sum_{n=1}^{N}\left(\mu\|\varepsilon(D_{\boldsymbol{u}}^{n+1})\|_{L^2(\Omega)}^2+\frac{1}{4\lambda}\|\alpha D_p^{n+1}-D_\xi^{n+1}\|_{L^2(\Omega)}^2\right)+\frac{K}{2}\Delta t\|\nabla e_p^{h,N+1}\|_{L^2(\Omega)}^2\\
&\leq \tilde{C}\Bigg[(\Delta t)^3\int_0^T\left(\|\partial_{tt}\boldsymbol{u}\|_{H^1(\Omega)}^2+\|\partial_{tt}\xi\|_{L^2(\Omega)}^2+\|\partial_{tt}p\|_{L^2(\Omega)}^2\right)ds\\
&+h^{2k}\Delta t\int_0^T\left(\|\partial_t\boldsymbol{u}\|_{H^{k+1}(\Omega)}^2+\|\partial_t\xi\|_{H^k(\Omega)}^2\right)ds+h^{2l+2}\Delta t\int_0^T\|\partial_t p\|_{H^{l+1}(\Omega)}^2ds\Bigg].
\end{aligned}\tag{38}$$

Here, $\tilde{C}=\tilde{C}(c_0,\lambda,\alpha)$.

Proof Subtracting (28), (29), (30) from (11), (12), (13), respectively, we derive

$$\begin{aligned}
&a_1(e_{\boldsymbol{u}}^{n+1},\boldsymbol{v}_h)-b(\boldsymbol{v}_h,e_\xi^{n+1})=0,\\
&b(e_{\boldsymbol{u}}^{n+1}-e_{\boldsymbol{u}}^n,\phi_h)+a_2(e_\xi^{n+1}-e_\xi^n,\phi_h)=c(p^{n+1}-p^n-p_h^n+p_h^{n-1},\phi_h),\\
&a_3\left(\partial_t p^{n+1}-\frac{p_h^{n+1}-p_h^n}{\Delta t},\psi_h\right)+d(e_p^{n+1},\psi_h)=c\left(\psi_h,\partial_t\xi^{n+1}-\frac{\xi_h^{n+1}-\xi_h^n}{\Delta t}\right).
\end{aligned}$$

By using the projection operators introduced in (16), (17), and (18), we can reformulate the above equations as

$$a_1(e_{\boldsymbol{u}}^{h,n+1},\boldsymbol{v}_h)-b(\boldsymbol{v}_h,e_\xi^{h,n+1})=0,\tag{39}$$

$$b(D_{\boldsymbol{u}}^{n+1},\phi_h)+a_2(e_\xi^{n+1}-e_\xi^n,\phi_h)=c(p^{n+1}-p^n-p_h^n+p_h^{n-1},\phi_h),\tag{40}$$

$$\begin{aligned}
&a_3(D_p^{n+1},\psi_h)-c(\psi_h,D_\xi^{n+1})+\Delta t d(e_p^{h,n+1},\psi_h)\\
&=a_3(R_p p^{n+1}-R_p p^n-\Delta t\partial_t p^{n+1},\psi_h)-c(\psi_h,R_\xi\xi^{n+1}-R_\xi\xi^n-\Delta t\partial_t\xi^{n+1}).
\end{aligned}\tag{41}$$

We take the difference of the $(n+1)$-th and the n-th levels of (39) to get

$$a_1(D_{\boldsymbol{u}}^{n+1},\boldsymbol{v}_h)-b(\boldsymbol{v}_h,D_\xi^{n+1})=0,\tag{42}$$

By using the definitions of D_ξ^{n+1} and D_p^n, we reformulate (40) as

$$\begin{aligned}
&b(D_{\boldsymbol{u}}^{n+1},\phi_h)+a_2(D_\xi^{n+1},\phi_h)-c(D_p^n,\phi_h)\\
&=-a_2(\xi^{n+1}-\xi^n,\phi_h)+c(p^{n+1}-p^n,\phi_h)\\
&\quad+a_2(R_\xi\xi^{n+1}-R_\xi\xi^n,\phi_h)-c(R_p p^n-R_p p^{n-1},\phi_h).
\end{aligned}\tag{43}$$

From (12) we obtain

$$b(\boldsymbol{u}^{n+1}-\boldsymbol{u}^n)=-a_2(\xi^{n+1}-\xi^n,\phi_h)+c(p^{n+1}-p^n,\phi_h),\tag{44}$$

$$b(\Delta t\partial_t\boldsymbol{u}^{n+1},\phi_h)+a_2(\Delta t\partial_t\xi^{n+1},\phi_h)-c(\Delta t\partial_t p^{n+1},\phi_h)=0.\tag{45}$$

Combining (43), (44), and (45) yields

$$b(D_{\boldsymbol{u}}^{n+1},\phi_h)+a_2(D_\xi^{n+1},\phi_h)-c(D_p^n,\phi_h)=b(\boldsymbol{u}^{n+1}-\boldsymbol{u}^n-\Delta t\partial_t\boldsymbol{u}^{n+1},\phi_h)$$
$$+a_2(R_\xi\xi^{n+1}-R_\xi\xi^n-\Delta t\partial_t\xi^{n+1},\phi_h)-c(R_pp^n-R_pp^{n-1}-\Delta t\partial_t p^{n+1},\phi_h). \quad (46)$$

Choosing $\boldsymbol{v}_h=D_{\boldsymbol{u}}^{n+1}$ in (42), $\phi_h=D_\xi^{n+1}$ in (46), and $\psi_h=D_p^{n+1}$ in (41), we deduce that

$$\begin{aligned}
&a_1(D_{\boldsymbol{u}}^{n+1},D_{\boldsymbol{u}}^{n+1})+a_2(D_\xi^{n+1},D_\xi^{n+1})+a_3(D_p^{n+1},D_p^{n+1})\\
&-c(D_p^{n+1},D_\xi^{n+1})+\Delta td(e_p^{h,n+1},D_p^{n+1})\\
&=b(\boldsymbol{u}^{n+1}-\boldsymbol{u}^n-\Delta t\partial_t\boldsymbol{u}^{n+1},D_\xi^{n+1})+a_2(R_\xi\xi^{n+1}-R_\xi\xi^n-\Delta t\partial_t\xi^{n+1},D_\xi^{n+1})\\
&+c(\Delta t\partial_t p^{n+1}-R_pp^n+R_pp^{n-1},D_\xi^{n+1})+a_3(R_pp^{n+1}-R_pp^n-\Delta t\partial_t p^{n+1},D_p^{n+1})\\
&+c(D_p^{n+1},\Delta t\partial_t\xi^{n+1}-R_\xi\xi^{n+1}+R_\xi\xi^n)+c(D_p^n,D_\xi^{n+1}). \quad (47)
\end{aligned}$$

From the definition of the bilinear form $c(\cdot,\cdot)$, the following identity holds.

$$\frac{1}{2\lambda}\|D_\xi^{n+1}\|_{L^2(\Omega)}^2+\frac{\alpha^2}{2\lambda}\|D_p^{n+1}\|_{L^2(\Omega)}^2-c(D_p^{n+1},D_\xi^{n+1})=\frac{1}{2\lambda}\|\alpha D_p^{n+1}-D_\xi^{n+1}\|_{L^2(\Omega)}^2. \quad (48)$$

Applying (48) to the left hand side of (47), and summing over the index n from 1 to N, we derive

$$\sum_{n=1}^{N}\left[2\mu\|\varepsilon(D_{\boldsymbol{u}}^{n+1})\|_{L^2(\Omega)}^2+\frac{1}{2\lambda}\|D_\xi^{n+1}\|_{L^2(\Omega)}^2+\left(c_0+\frac{\alpha^2}{2\lambda}\right)\|D_p^{n+1}\|_{L^2(\Omega)}^2\right.$$
$$\left.+\frac{1}{2\lambda}\|\alpha D_p^{n+1}-D_\xi^{n+1}\|_{L^2(\Omega)}^2\right]+\Delta t\sum_{n=1}^{N}d(e_p^{h,n+1},D_p^{n+1})=\sum_{i=1}^{6}T_i, \quad (49)$$

where

$$T_1=\sum_{n=1}^{N}b(\boldsymbol{u}^{n+1}-\boldsymbol{u}^n-\Delta t\partial_t\boldsymbol{u}^{n+1},D_\xi^{n+1}),$$
$$T_2=\sum_{n=1}^{N}a_2(R_\xi\xi^{n+1}-R_\xi\xi^n-\Delta t\partial_t\xi^{n+1},D_\xi^{n+1}),$$
$$T_3=\sum_{n=1}^{N}c(\Delta t\partial_t p^{n+1}-R_pp^n+R_pp^{n-1},D_\xi^{n+1}),$$
$$T_4=\sum_{n=1}^{N}a_3(R_pp^{n+1}-R_pp^n-\Delta t\partial_t p^{n+1},D_p^{n+1}),$$
$$T_5=\sum_{n=1}^{N}c(D_p^{n+1},\Delta t\partial_t\xi^{n+1}-R_\xi\xi^{n+1}+R_\xi\xi^n),$$
$$T_6=\sum_{n=1}^{N}c(D_p^n,D_\xi^{n+1}).$$

Next, we bound the terms T_i for $i = 1, 2, \ldots, 6$. Recalling the definition of $b(\cdot, \cdot)$, we can apply the Cauchy-Schwarz inequality, Young's inequality to derive the following estimate for the term T_1 with any $\epsilon_1 > 0$.

$$\begin{aligned} T_1 &= \sum_{n=1}^{N} \int_{\Omega} D_{\xi}^{n+1} \operatorname{div}(\boldsymbol{u}^{n+1} - \boldsymbol{u}^n - \Delta t \partial_t \boldsymbol{u}^{n+1}) \\ &\leq \frac{\epsilon_1}{3} \sum_{n=1}^{N} \| D_{\xi}^{n+1} \|_{L^2(\Omega)}^2 + \frac{C}{\epsilon_1} \sum_{n=1}^{N} \| \operatorname{div}(\boldsymbol{u}^{n+1} - \boldsymbol{u}^n - \Delta t \partial_t \boldsymbol{u}^{n+1}) \|_{L^2(\Omega)}^2. \end{aligned}$$

Then, we can apply (36) to control the last item as follows.

$$T_1 \leq \frac{\epsilon_1}{3} \sum_{n=1}^{N} \| D_{\xi}^{n+1} \|_{L^2(\Omega)}^2 + \frac{C}{\epsilon_1} (\Delta t)^3 \int_0^T \| \partial_{tt} \boldsymbol{u} \|_{H^1(\Omega)}^2 ds.$$

Considering the same ϵ_1, we then estimate the T_2 term in the same manner.

$$\begin{aligned} T_2 &= \sum_{n=1}^{N} \frac{1}{\lambda} \int_{\Omega} D_{\xi}^{n+1} (R_{\xi} \xi^{n+1} - R_{\xi} \xi^n - \Delta t \partial_t \xi^{n+1}) \\ &\leq \frac{\epsilon_1}{3} \sum_{n=1}^{N} \| D_{\xi}^{n+1} \|_{L^2}^2 + \frac{C}{\epsilon_1 \lambda^2} \sum_{n=1}^{N} \| R_{\xi} \xi^{n+1} - R_{\xi} \xi^n - \Delta t \partial_t \xi^{n+1} \|_{L^2(\Omega)}^2 \\ &\leq \frac{\epsilon_1}{3} \sum_{n=1}^{N} \| D_{\xi}^{n+1} \|_{L^2}^2 + \frac{C}{\epsilon_1 \lambda^2} \sum_{n=1}^{N} \Big(\| \xi^{n+1} - \xi^n - \Delta t \partial_t \xi^{n+1} \|_{L^2(\Omega)}^2 \\ &\quad + \| R_{\xi} (\xi^{n+1} - \xi^n) - (\xi^{n+1} - \xi^n) \|_{L^2(\Omega)}^2 \Big). \end{aligned}$$

Applying (36) and (19), we can bound T_2 as follows.

$$\begin{aligned} T_2 \leq \frac{\epsilon_1}{3} \sum_{n=1}^{N} \| D_{\xi}^{n+1} \|_{L^2(\Omega)}^2 + \frac{C}{\epsilon_1 \lambda^2} \Big[(\Delta t)^3 \int_0^T \| \partial_{tt} \xi \|_{L^2(\Omega)}^2 ds \\ + h^{2k} \Delta t \int_0^T \left(\| \partial_t \boldsymbol{u} \|_{H^{k+1}(\Omega)}^2 + \| \partial_t \xi \|_{H^k(\Omega)}^2 \right) ds \Big]. \end{aligned}$$

To estimate the term T_3, we need to reformulate it first.

$$\begin{aligned} T_3 &= \sum_{n=1}^{N} \Big[c(\Delta t \partial_t p^{n+1} - \Delta t \partial_t p^n, D_{\xi}^{n+1}) + c(\Delta t \partial_t p^n - R_p p^n + R_p p^{n-1}, D_{\xi}^{n+1}) \Big] \\ &= \sum_{n=1}^{N} \frac{\alpha}{\lambda} \int_{\Omega} D_{\xi}^{n+1} (\Delta t \partial_t p^{n+1} - \Delta t \partial_t p^n) + \sum_{n=1}^{N} \frac{\alpha}{\lambda} \int_{\Omega} D_{\xi}^{n+1} (\Delta t \partial_t p^n - R_p p^n + R_p p^{n-1}) \\ &\leq \frac{\epsilon_1}{3} \sum_{n=1}^{N} \| D_{\xi}^{n+1} \|_{L^2(\Omega)}^2 + \frac{C\alpha^2}{\epsilon_1 \lambda^2} \sum_{n=1}^{N} \Big(\| \Delta t \partial_t p^{n+1} - \Delta t \partial_t p^n \|_{L^2(\Omega)}^2 \\ &\quad + \| p^n - p^{n-1} - \Delta t \partial_t p^n \|_{L^2(\Omega)}^2 + \| R_p (p^n - p^{n-1}) - (p^n - p^{n-1}) \|_{L^2(\Omega)}^2 \Big). \end{aligned}$$

We then apply (36) and (21) to derive the following estimate.

$$T_3 \le \frac{\epsilon_1}{3}\sum_{n=1}^{N}\|D_\xi^{n+1}\|_{L^2(\Omega)}^2 + \frac{C\alpha^2}{\epsilon_1\lambda^2}\left[(\Delta t)^3\int_0^T \|\partial_{tt}p\|_{L^2(\Omega)}^2 ds + h^{2l+2}\Delta t\int_0^T \|\partial_t p\|_{H^{l+1}(\Omega)}^2 ds\right].$$

Similarly, we recall the definition of $a_3(\cdot,\cdot)$ to derive the following estimate for the term T_4 with any $\epsilon_2 > 0$.

$$\begin{aligned}
T_4 &= \sum_{n=1}^{N}\left(c_0 + \frac{\alpha^2}{\lambda}\right)\int_\Omega D_p^{n+1}(R_p p^{n+1} - R_p p^n - \Delta t\partial_t p^{n+1}) \\
&\le c_0\sum_{n=1}^{N}\|D_p^{n+1}\|_{L^2(\Omega)}^2 + \frac{\epsilon_2\alpha^2}{4}\sum_{n=1}^{N}\|D_p^{n+1}\|_{L^2(\Omega)}^2 \\
&\quad + C\left(c_0 + \frac{\alpha^2}{\epsilon_2\lambda^2}\right)\left[(\Delta t)^3\int_0^T \|\partial_{tt}p\|_{L^2(\Omega)}^2 ds + h^{2l+2}\Delta t\int_0^T \|\partial_t p\|_{H^{l+1}(\Omega)}^2 ds\right].
\end{aligned}$$

Using the same technique, we can bound T_5 and T_6 as follows.

$$\begin{aligned}
T_5 &= \sum_{n=1}^{N}\frac{\alpha}{\lambda}\int_\Omega D_p^{n+1}(\Delta t\partial_t\xi^{n+1} - R_\xi\xi^{n+1} + R_\xi\xi^n) \\
&\le \frac{\epsilon_2\alpha^2}{4}\sum_{n=1}^{N}\|D_p^{n+1}\|_{L^2(\Omega)}^2 + \frac{C}{\epsilon_2\lambda^2}\left[(\Delta t)^3\int_0^T \|\partial_{tt}\xi\|_{L^2(\Omega)}^2 ds\right. \\
&\quad \left. + h^{2k}\Delta t\int_0^T \left(\|\partial_t\boldsymbol{u}\|_{H^{k+1}(\Omega)}^2 + \|\partial_t\xi\|_{H^k(\Omega)}^2\right) ds\right], \\
T_6 &= \sum_{n=1}^{N}\frac{\alpha}{\lambda}\int_\Omega D_\xi^{n+1}D_p^n \le \frac{1}{2\lambda}\sum_{n=1}^{N}\|D_\xi^{n+1}\|_{L^2(\Omega)}^2 + \frac{\alpha^2}{2\lambda}\sum_{n=1}^{N}\|D_p^n\|_{L^2(\Omega)}^2.
\end{aligned}$$

From (37), we also have the following inequality.

$$\begin{aligned}
\Delta t\sum_{n=1}^{N} d(e_p^{h,n+1}, D_p^{n+1}) &\ge \Delta t\sum_{n=1}^{N}\left(\frac{K}{2}\|\nabla e_p^{h,n+1}\|_{L^2(\Omega)}^2 - \frac{K}{2}\|\nabla e_p^{h,n}\|_{L^2(\Omega)}^2\right) \\
&= \frac{K}{2}\Delta t\|\nabla e_p^{h,N+1}\|_{L^2(\Omega)}^2 - \frac{K}{2}\Delta t\|\nabla e_p^{h,1}\|_{L^2(\Omega)}^2. \qquad (50)
\end{aligned}$$

We denote $\tilde{C}$ a constant related to ϵ_1, ϵ_2 and other coefficients, which will be discussed later. Combining (49), (50), and the bounds of T_i for $i = 1, 2, \ldots, 6$, we obtain

$$\begin{aligned}
&\sum_{n=1}^{N}\left[2\mu\|\varepsilon(D_{\boldsymbol{u}}^{n+1})\|_{L^2(\Omega)}^2 + \frac{\alpha^2}{2\lambda}\|D_p^{n+1}\|_{L^2(\Omega)}^2 + \frac{1}{2\lambda}\|\alpha D_p^{n+1} - D_\xi^{n+1}\|_{L^2(\Omega)}^2\right] \\
&\quad + \frac{K}{2}\Delta t\|\nabla e_p^{h,N+1}\|_{L^2(\Omega)}^2 - \frac{K}{2}\Delta t\|\nabla e_p^{h,1}\|_{L^2(\Omega)}^2 \\
&\quad \le \epsilon_1\sum_{n=1}^{N}\|D_\xi^{n+1}\|_{L^2(\Omega)}^2 + \frac{\epsilon_2\alpha^2}{2}\sum_{n=1}^{N}\|D_p^{n+1}\|_{L^2(\Omega)}^2 + \frac{\alpha^2}{2\lambda}\sum_{n=1}^{N}\|D_p^n\|_{L^2(\Omega)}^2 \\
&\quad + \tilde{C}\left[(\Delta t)^3\int_0^T \left(\|\partial_{tt}\boldsymbol{u}\|_{H^1(\Omega)}^2 + \|\partial_{tt}\xi\|_{L^2(\Omega)}^2 + \|\partial_{tt}p\|_{L^2(\Omega)}^2\right) ds\right.
\end{aligned}$$

$$+ h^{2k}\Delta t \int_0^T \left(\|\partial_t \boldsymbol{u}\|^2_{H^{k+1}(\Omega)} + \|\partial_t \xi\|^2_{H^k(\Omega)} \right) ds + h^{2l+2}\Delta t \int_0^T \|\partial_t p\|^2_{H^{l+1}(\Omega)} ds \Bigg]. \tag{51}$$

Using the inf-sup condition (15), (42) yields

$$\tilde{\beta}\|D_\xi^{n+1}\|^2_{L^2(\Omega)} \le \sup_{\boldsymbol{v}_h \in \boldsymbol{V}_h} \frac{b(\boldsymbol{v}_h, D_\xi^{n+1})}{\|\boldsymbol{v}_h\|_{H^1(\Omega)}} = \sup_{\boldsymbol{v}_h \in \boldsymbol{V}_h} \frac{a_1(D_{\boldsymbol{u}}^{n+1}, \boldsymbol{v}_h)}{\|\boldsymbol{v}_h\|_{H^1(\Omega)}} \le 2\mu C_1 \|\varepsilon(D_{\boldsymbol{u}}^{n+1})\|^2_{L^2(\Omega)}, \tag{52}$$

which directly implies

$$\begin{aligned} \frac{\alpha^2}{2}\|D_p^{n+1}\|^2_{L^2(\Omega)} &\le \|\alpha D_p^{n+1} - D_\xi^{n+1}\|^2_{L^2(\Omega)} + \|D_\xi^{n+1}\|^2_{L^2(\Omega)} \\ &\le \|\alpha D_p^{n+1} - D_\xi^{n+1}\|^2_{L^2(\Omega)} + \frac{2\mu C_1}{\tilde{\beta}}\|\varepsilon(D_{\boldsymbol{u}}^{n+1})\|^2_{L^2(\Omega)}. \end{aligned} \tag{53}$$

According to (52), we determine coefficient $\epsilon_1 = \frac{\tilde{\beta}}{4C_1}$ such that $\epsilon_1\|D_\xi^{n+1}\|^2_{L^2(\Omega)} \le \frac{\mu}{2}\|\varepsilon(D_{\boldsymbol{u}}^{n+1})\|^2_{L^2(\Omega)}$. And we recall (53) to set $\epsilon_2 = \min\{\frac{1}{4\lambda}, \frac{\tilde{\beta}}{4C_1}\}$ such that $\frac{\epsilon_2\alpha^2}{2}\|D_p^{n+1}\|^2_{L^2(\Omega)} \le \frac{\mu}{2}\|\varepsilon(D_{\boldsymbol{u}}^{n+1})\|^2_{L^2(\Omega)} + \frac{1}{4\lambda}\|\alpha D_p^{n+1} - D_\xi^{n+1}\|^2_{L^2(\Omega)}$. From (51), we see that

$$\begin{aligned} &\sum_{n=1}^N \left(\mu\|\varepsilon(D_{\boldsymbol{u}}^{n+1})\|^2_{L^2(\Omega)} + \frac{1}{4\lambda}\|\alpha D_p^{n+1} - D_\xi^{n+1}\|^2_{L^2(\Omega)} \right) + \frac{K}{2}\Delta t\|\nabla e_p^{h,N+1}\|^2_{L^2(\Omega)} \\ &\le \tilde{C}\Bigg[(\Delta t)^3 \int_0^T \left(\|\partial_{tt}\boldsymbol{u}\|^2_{H^1(\Omega)} + \|\partial_{tt}\xi\|^2_{L^2(\Omega)} + \|\partial_{tt} p\|^2_{L^2(\Omega)} \right) ds \\ &+ h^{2k}\Delta t \int_0^T \left(\|\partial_t \boldsymbol{u}\|^2_{H^{k+1}(\Omega)} + \|\partial_t \xi\|^2_{H^k(\Omega)} \right) ds \\ &+ h^{2l+2}\Delta t \int_0^T \|\partial_t p\|^2_{H^{l+1}(\Omega)} ds \Bigg] + \frac{\alpha^2}{2\lambda}\|D_p^1\|^2_{L^2(\Omega)} + \frac{K}{2}\Delta t\|\nabla e_p^{h,1}\|^2_{L^2(\Omega)}. \end{aligned}$$

We then apply (34) to handle the last two terms on the right-hand side. When $c_0 \to 0$, $\lambda \to \infty$, the constant $\tilde{C}$ exhibits robustness with respect to c_0, λ, and α because

$$\tilde{C} = \tilde{C}(c_0, \lambda, \alpha) \lesssim 1 + c_0 + \frac{1+\alpha^2}{\lambda} + \frac{1+\alpha^2}{\lambda^2}.$$

The proof of (38) is completed. □

Theorem 3 *Let* $(\boldsymbol{u}, \xi, p)$ *and* $(\boldsymbol{u}_h^{n+1}, \xi_h^{n+1}, p_h^{n+1})$ *for* $n \ge 1$ *be the solutions of Eqs.* (11)–(13) *and Eqs.* (28)–(30)*, respectively. Under* ***Assumption*** 1*, there holds*

$$\begin{aligned} &\mu\|\varepsilon(e_{\boldsymbol{u}}^{h,N+1})\|^2_{L^2(\Omega)} + \|e_\xi^{h,N+1}\|^2_{L^2(\Omega)} + \left(c_0 + \frac{\alpha^2}{\lambda} \right)\|e_p^{h,N+1}\|^2_{L^2(\Omega)} \\ &+ K\Delta t \sum_{n=1}^N \|\nabla e_p^{h,n+1}\|^2_{L^2(\Omega)} \\ &\le \tilde{C}\Bigg[(\Delta t)^2 \int_0^T \left(\|\partial_{tt}\boldsymbol{u}\|^2_{H^1(\Omega)} + \|\partial_{tt}\xi\|^2_{L^2(\Omega)} + \|\partial_{tt} p\|^2_{L^2(\Omega)} \right) ds \end{aligned}$$

$$+ h^{2k} \int_0^T \left(\|\partial_t \boldsymbol{u}\|^2_{H^{k+1}(\Omega)} + \|\partial_t \xi\|^2_{H^k(\Omega)} \right) ds + h^{2l+2} \int_0^T \|\partial_t p\|^2_{H^{l+1}(\Omega)} ds \Big]. \quad (54)$$

Here, $\tilde{C} = \tilde{C}(T, c_0, \lambda, \alpha)$.

Proof Choosing $\boldsymbol{v}_h = D_{\boldsymbol{u}}^{n+1}$ in (39), $\phi_h = e_\xi^{h,n+1}$ in (46) and $\psi_h = e_p^{h,n+1}$ in (41) yields

$$a_1(e_{\boldsymbol{u}}^{h,n+1}, D_{\boldsymbol{u}}^{n+1}) - b(D_{\boldsymbol{u}}^{n+1}, e_\xi^{h,n+1}) = 0, \quad (55)$$

$$\begin{aligned} &b(D_{\boldsymbol{u}}^{n+1}, e_\xi^{h,n+1}) + a_2(D_\xi^{n+1}, e_\xi^{h,n+1}) - c(D_p^{n+1}, e_\xi^{h,n+1}) \\ &= b(\boldsymbol{u}^{n+1} - \boldsymbol{u}^n - \Delta t \partial_t \boldsymbol{u}^{n+1}, e_\xi^{h,n+1}) \\ &\quad + a_2(R_\xi \xi^{n+1} - R_\xi \xi^n - \Delta t \partial_t \xi^{n+1}, e_\xi^{h,n+1}) \\ &\quad - c(R_p p^n - R_p p^{n-1} - \Delta t \partial_t p^{n+1}, e_\xi^{h,n+1}) - c(D_p^{n+1} - D_p^n, e_\xi^{h,n+1}), \end{aligned} \quad (56)$$

$$\begin{aligned} &a_3(D_p^{n+1}, e_p^{h,n+1}) - c(e_p^{h,n+1}, D_\xi^{n+1}) + \Delta t d(e_p^{h,n+1}, e_p^{h,n+1}) \\ &= a_3(R_p p^{n+1} - R_p p^n - \Delta t \partial_t p^{n+1}, e_p^{h,n+1}) \\ &\quad - c(e_p^{h,n+1}, R_\xi \xi^{n+1} - R_\xi \xi^n - \Delta t \partial_t \xi^{n+1}). \end{aligned} \quad (57)$$

Then, we take the summation of (55), (56), and (57) over the index n from 1 to N

$$\begin{aligned} \text{LHS} := \sum_{n=1}^N \Big[&a_1(e_{\boldsymbol{u}}^{h,n+1}, D_{\boldsymbol{u}}^{n+1}) + a_2(D_\xi^{n+1}, e_\xi^{h,n+1}) - c(D_p^{n+1}, e_\xi^{h,n+1}) \\ &+ a_3(D_p^{n+1}, e_p^{h,n+1}) - c(e_p^{h,n+1}, D_\xi^{n+1}) + \Delta t d(e_p^{h,n+1}, e_p^{h,n+1}) \Big] = \sum_{i=1}^6 E_i, \end{aligned} \quad (58)$$

where

$$\begin{aligned} E_1 &= \sum_{n=1}^N b(\boldsymbol{u}^{n+1} - \boldsymbol{u}^n - \Delta t \partial_t \boldsymbol{u}^{n+1}, e_\xi^{h,n+1}), \\ E_2 &= \sum_{n=1}^N a_2(R_\xi \xi^{n+1} - R_\xi \xi^n - \Delta t \partial_t \xi^{n+1}, e_\xi^{h,n+1}), \\ E_3 &= \sum_{n=1}^N c(\Delta t \partial_t p^{n+1} - R_p p^n + R_p p^{n-1}, e_\xi^{h,n+1}), \\ E_4 &= \sum_{n=1}^N a_3(R_p p^{n+1} - R_p p^n - \Delta t \partial_t p^{n+1}, e_p^{h,n+1}), \\ E_5 &= \sum_{n=1}^N c(e_p^{h,n+1}, \Delta t \partial_t \xi^{n+1} - R_\xi \xi^{n+1} + R_\xi \xi^n), \\ E_6 &= \sum_{n=1}^N c(D_p^{n+1} - D_p^n, -e_\xi^{h,n+1}). \end{aligned}$$

Using the definitions of $a_2(\cdot,\cdot)$, $a_3(\cdot,\cdot)$ and $c(\cdot,\cdot)$, we have the following identity.

$$a_2(D_\xi^{n+1}, e_\xi^{h,n+1}) - c(D_p^{n+1}, e_\xi^{h,n+1}) + a_3(D_p^{n+1}, e_p^{h,n+1}) - c(e_p^{h,n+1}, D_\xi^{n+1})$$

$$= \frac{1}{\lambda}\int_\Omega (\alpha D_p^{n+1} - D_\xi^{n+1})(\alpha e_p^{h,n+1} - e_\xi^{h,n+1}) + c_0\int_\Omega (e_p^{h,n+1} - e_p^{h,n}) e_p^{h,n+1}. \quad (59)$$

Applying (37) and (59) to (58), we can estimate that

$$\sum_{n=1}^{N}\Bigg(\mu\|\varepsilon(e_{\boldsymbol{u}}^{h,n+1})\|_{L^2(\Omega)}^2 - \mu\|\varepsilon(e_{\boldsymbol{u}}^{h,n})\|_{L^2(\Omega)}^2 + \frac{c_0}{2}\|e_p^{h,n+1}\|_{L^2(\Omega)}^2 - \frac{c_0}{2}\|e_p^{h,n}\|_{L^2(\Omega)}^2 + \frac{1}{2\lambda}\|\alpha e_p^{h,n+1} - e_\xi^{h,n+1}\|_{L^2(\Omega)}^2 - \frac{1}{2\lambda}\|\alpha e_p^{h,n} - e_\xi^{h,n}\|_{L^2(\Omega)}^2 + K\Delta t\|\nabla e_p^{h,n+1}\|_{L^2(\Omega)}^2\Bigg) \le \text{LHS},$$

which directly implies that

$$\frac{1}{2}\Bigg(2\mu\|\varepsilon(e_{\boldsymbol{u}}^{h,N+1})\|_{L^2(\Omega)}^2 - 2\mu\|\varepsilon(e_{\boldsymbol{u}}^{h,1})\|_{L^2(\Omega)}^2 + c_0\|e_p^{h,N+1}\|_{L^2(\Omega)}^2 - c_0\|e_p^{h,1}\|_{L^2(\Omega)}^2 + \frac{1}{\lambda}\|\alpha e_p^{h,N+1} - e_\xi^{h,N+1}\|_{L^2(\Omega)}^2 - \frac{1}{\lambda}\|\alpha e_p^{h,1} - e_\xi^{h,1}\|_{L^2(\Omega)}^2\Bigg) + K\Delta t\sum_{n=1}^{N}\|\nabla e_p^{h,n+1}\|_{L^2(\Omega)}^2 \le \text{LHS}. \quad (60)$$

Next, we bound the terms E_i for $i = 1, 2, \ldots, 6$. We use the Cauchy-Schwarz inequality, Young's inequality, (19), (21) and (36) to estimate E_1, E_2, and E_3 with any $\epsilon_1 > 0$ as follows.

$$E_1 \le \frac{\epsilon_1}{6}\Delta t\sum_{n=1}^{N}\|e_\xi^{h,n+1}\|_{L^2(\Omega)}^2 + \frac{C}{\epsilon_1}(\Delta t)^2\int_0^T \|\partial_{tt}\boldsymbol{u}\|_{H^1(\Omega)}^2 ds,$$

$$E_2 \le \frac{\epsilon_1}{6}\Delta t\sum_{n=1}^{N}\|e_\xi^{h,n+1}\|_{L^2(\Omega)}^2 + \frac{C}{\epsilon_1\lambda^2}\Bigg[(\Delta t)^2\int_0^T \|\partial_{tt}\xi\|_{L^2(\Omega)}^2 ds + h^{2k}\int_0^T \left(\|\partial_t\boldsymbol{u}\|_{H^{k+1}(\Omega)}^2 + \|\partial_t\xi\|_{H^k(\Omega)}^2\right) ds\Bigg],$$

$$E_3 = \sum_{n=1}^{N}\Big[c(\Delta t\,\partial_t p^{n+1} - \Delta t\,\partial_t p^n, e_\xi^{h,n+1}) + c(\Delta t\,\partial_t p^n - R_p p^n + R_p p^{n-1}, e_\xi^{h,n+1})\Big]$$
$$\le \frac{\epsilon_1}{6}\Delta t\sum_{n=1}^{N}\|e_\xi^{h,n+1}\|_{L^2(\Omega)}^2 + \frac{C\alpha^2}{\epsilon_1\lambda^2}\Bigg[(\Delta t)^2\int_0^T \|\partial_{tt}p\|_{L^2(\Omega)}^2 ds + h^{2l+2}\int_0^T \|\partial_t p\|_{H^{l+1}(\Omega)}^2 ds\Bigg].$$

Using the Cauchy-Schwarz inequality, Young's inequality, (19), (21), and (36), we can bound E_4 and E_5 with any $\epsilon_2 > 0$ as follows.

$$E_4 \le \frac{c_0}{2}\Delta t\sum_{n=1}^{N}\|e_p^{h,n+1}\|_{L^2(\Omega)}^2 + \frac{\epsilon_2\alpha^2}{8}\Delta t\sum_{n=1}^{N}\|e_p^{h,n+1}\|_{L^2(\Omega)}^2 + C\left(c_0 + \frac{\alpha^2}{\epsilon_2\lambda^2}\right)\Bigg[(\Delta t)^2\int_0^T \|\partial_{tt}p\|_{L^2(\Omega)}^2 ds + h^{2l+2}\int_0^T \|\partial_t p\|_{H^{l+1}(\Omega)}^2 ds\Bigg],$$

$$E_5 \le \frac{\epsilon_2\alpha^2}{8}\Delta t\sum_{n=1}^{N}\|e_p^{h,n+1}\|_{L^2(\Omega)}^2 + \frac{C}{\epsilon_2\lambda^2}\Big[(\Delta t)^2\int_0^T \|\partial_{tt}\xi\|_{L^2(\Omega)}^2 ds + h^{2k}\int_0^T \Big(\|\partial_t \boldsymbol{u}\|_{H^{k+1}(\Omega)}^2 + \|\partial_t\xi\|_{H^k(\Omega)}^2\Big) ds\Big].$$

Then, we estimate the term E_6 with any $\epsilon_3 > 0$ as follows.

$$\begin{aligned} E_6 &= \sum_{n=1}^{N}\Big[-c(D_p^{n+1}, e_\xi^{h,n+1}) + c(D_p^n, D_\xi^{n+1}) + c(D_p^n, e_\xi^{h,n})\Big] \\ &= -c(D_p^{N+1}, e_\xi^{h,N+1}) + \sum_{n=1}^{N} c(D_p^n, D_\xi^{n+1}) + c(D_p^1, e_\xi^{h,1}) \\ &\le \sum_{n=1}^{N}\Big(\frac{\alpha^2}{2\lambda}\|D_p^{n+1}\|_{L^2(\Omega)}^2 + \frac{1}{2\lambda}\|D_\xi^{n+1}\|_{L^2(\Omega)}^2\Big) + \frac{\alpha^2}{\epsilon_3 2\lambda^2}\|D_p^{N+1}\|_{L^2(\Omega)}^2 \\ &\quad + \frac{\epsilon_3}{2}\|e_\xi^{h,N+1}\|_{L^2(\Omega)}^2 + \frac{\alpha^2}{\lambda}\|D_p^1\|_{L^2(\Omega)}^2 + \frac{1}{2\lambda}\|e_\xi^{h,1}\|_{L^2(\Omega)}^2. \end{aligned}$$

Again, we denote $\tilde{C}$ a constant related to ϵ_1, ϵ_2 and other coefficients, which will be discussed later. Combining the bounds of E_i for $i = 1, 2, \ldots, 6$, together with (58), we derive that

$$\begin{aligned} &2\mu\|\varepsilon(e_{\boldsymbol{u}}^{h,N+1})\|_{L^2(\Omega)}^2 - 2\mu\|\varepsilon(e_{\boldsymbol{u}}^{h,1})\|_{L^2(\Omega)}^2 + c_0\|e_p^{h,N+1}\|_{L^2(\Omega)}^2 - c_0\|e_p^{h,1}\|_{L^2(\Omega)}^2 \\ &\quad + \frac{1}{\lambda}\|\alpha e_p^{h,N+1} - e_\xi^{h,N+1}\|_{L^2(\Omega)}^2 - \frac{1}{\lambda}\|\alpha e_p^{h,1} - e_\xi^{h,1}\|_{L^2(\Omega)}^2 + 2K\Delta t\sum_{n=1}^{N}\|\nabla e_p^{h,n+1}\|_{L^2(\Omega)}^2 \\ &\quad \le \epsilon_1\Delta t\sum_{n=1}^{N}\|e_\xi^{h,n+1}\|_{L^2(\Omega)}^2 + c_0\Delta t\sum_{n=1}^{N}\|e_p^{h,n+1}\|_{L^2(\Omega)}^2 + \frac{\epsilon_2\alpha^2}{2}\Delta t\sum_{n=1}^{N}\|e_p^{h,n+1}\|_{L^2(\Omega)}^2 \\ &\quad + \epsilon_3\|e_\xi^{h,N+1}\|_{L^2(\Omega)}^2 + \sum_{n=1}^{N}\frac{\alpha^2}{\lambda}\|D_p^{n+1}\|_{L^2(\Omega)}^2 + \sum_{n=1}^{N}\frac{1}{\lambda}\|D_\xi^{n+1}\|_{L^2(\Omega)}^2 + \frac{\alpha^2}{\epsilon_3\lambda^2}\|D_p^{N+1}\|_{L^2(\Omega)}^2 \\ &\quad + \tilde{C}\Big[(\Delta t)^2\int_0^T\Big(\|\partial_{tt}\boldsymbol{u}\|_{H^1(\Omega)}^2 + \|\partial_{tt}\xi\|_{L^2(\Omega)}^2 + \|\partial_{tt}p\|_{L^2(\Omega)}^2\Big) ds \\ &\quad + h^{2k}\int_0^T\Big(\|\partial_t\boldsymbol{u}\|_{H^{k+1}(\Omega)}^2 + \|\partial_t\xi\|_{H^k(\Omega)}^2\Big) ds + h^{2l+2}\int_0^T\|\partial_t p\|_{H^{l+1}(\Omega)}^2 ds\Big] \\ &\quad + \frac{2\alpha^2}{\lambda}\|D_p^1\|_{L^2(\Omega)}^2 + \frac{1}{\lambda}\|e_\xi^{h,1}\|_{L^2(\Omega)}^2, \end{aligned} \tag{61}$$

Using the inf-sup condition (15), (39) yields

$$\tilde{\beta}\|e_\xi^{h,n+1}\|_{L^2(\Omega)}^2 \le \sup_{\boldsymbol{v}_h\in\boldsymbol{V}_h}\frac{b(\boldsymbol{v}_h, e_\xi^{h,n+1})}{\|\boldsymbol{v}_h\|_{H^1(\Omega)}} = \sup_{\boldsymbol{v}_h\in\boldsymbol{V}_h}\frac{a_1(e_{\boldsymbol{u}}^{h,n+1}, \boldsymbol{v}_h)}{\|\boldsymbol{v}_h\|_{H^1(\Omega)}} \le 2\mu C_1\|\varepsilon(e_{\boldsymbol{u}}^{h,n+1})\|_{L^2(\Omega)}^2, \tag{62}$$

which easily implies that

$$\frac{\alpha^2}{2}\|e_p^{h,n+1}\|_{L^2(\Omega)}^2 \le \|\alpha e_p^{h,n+1} - e_\xi^{h,n+1}\|_{L^2(\Omega)}^2 + \|e_\xi^{h,n+1}\|_{L^2(\Omega)}^2$$

$$\leq \|\alpha e_p^{h,n+1} - e_\xi^{h,n+1}\|^2_{L^2(\Omega)} + \frac{2\mu C_1}{\tilde{\beta}}\|\varepsilon(e_{\boldsymbol{u}}^{h,n+1})\|^2_{L^2(\Omega)}. \tag{63}$$

First, we set $\epsilon_1 = \frac{\tilde{\beta}}{4C_1}$ such that $\epsilon_1\|e_\xi^{h,n+1}\|^2_{L^2(\Omega)} \leq \frac{\mu}{2}\|\varepsilon(e_{\boldsymbol{u}}^{h,n+1})\|^2_{L^2(\Omega)}$, $\epsilon_2 = \min\{\frac{1}{\lambda}, \frac{\tilde{\beta}}{4C_1}\}$ such that $\frac{\epsilon_2\alpha^2}{2}\|e_p^{h,n+1}\|^2_{L^2(\Omega)} \leq \frac{1}{\lambda}\|\alpha e_p^{h,n+1} - e_\xi^{h,n+1}\|^2_{L^2(\Omega)} + \frac{\mu}{2}\|\varepsilon(e_{\boldsymbol{u}}^{h,n+1})\|^2_{L^2(\Omega)}$, $\epsilon_3 = \frac{\tilde{\beta}}{2C_1}$ such that $\epsilon_3\|e_\xi^{h,N+1}\|^2_{L^2(\Omega)} \leq \mu\|\varepsilon(e_{\boldsymbol{u}}^{h,N+1})\|^2_{L^2(\Omega)}$. Then, we apply (38) to bound the summation of the $\|D_p^{n+1}\|^2_{L^2(\Omega)}$, $\|D_\xi^{n+1}\|^2_{L^2(\Omega)}$ terms. Additionally, we can use (34) and (35) to bound the last two terms $\|D_p^1\|^2_{L^2(\Omega)}$ and $\|e_\xi^{h,1}\|^2_{L^2(\Omega)}$ in the first time step $t = t_1$, and reformulate (61) as follows.

$$\begin{aligned}
&\mu\|\varepsilon(e_{\boldsymbol{u}}^{h,N+1})\|^2_{L^2(\Omega)} + c_0\|e_p^{h,N+1}\|^2_{L^2(\Omega)} + \frac{1}{\lambda}\|\alpha e_p^{h,N+1} - e_\xi^{h,N+1}\|^2_{L^2(\Omega)} \\
&\quad + 2K\Delta t\sum_{n=1}^{N}\|\nabla e_p^{h,n+1}\|^2_{L^2(\Omega)} \\
&\quad \leq \Delta t\sum_{n=1}^{N}\left(\mu\|\varepsilon(e_{\boldsymbol{u}}^{h,n+1})\|^2_{L^2(\Omega)} + c_0\|e_p^{h,n+1}\|^2_{L^2(\Omega)} + \frac{1}{\lambda}\|\alpha e_p^{h,n+1} - e_\xi^{h,n+1}\|^2_{L^2(\Omega)}\right) \\
&\quad + \tilde{C}\Bigg[(\Delta t)^2\int_0^T\left(\|\partial_{tt}\boldsymbol{u}\|^2_{H^1(\Omega)} + \|\partial_{tt}\xi\|^2_{L^2(\Omega)} + \|\partial_{tt}p\|^2_{L^2(\Omega)}\right)ds \\
&\quad + h^{2k}\int_0^T\left(\|\partial_t\boldsymbol{u}\|^2_{H^{k+1}(\Omega)} + \|\partial_t\xi\|^2_{H^k(\Omega)}\right)ds + h^{2l+2}\int_0^T\|\partial_t p\|^2_{H^{l+1}(\Omega)}ds\Bigg].
\end{aligned}$$

Finally, we apply the discrete Grönwall's inequality to obtain

$$\begin{aligned}
&\mu\|\varepsilon(e_{\boldsymbol{u}}^{h,N+1})\|^2_{L^2(\Omega)} + c_0\|e_p^{h,N+1}\|^2_{L^2(\Omega)} + \frac{1}{\lambda}\|\alpha e_p^{h,N+1} - e_\xi^{h,N+1}\|^2_{L^2(\Omega)} \\
&\quad + 2K\Delta t\sum_{n=1}^{N}\|\nabla e_p^{h,n+1}\|^2_{L^2(\Omega)} \\
&\quad \leq \tilde{C}\Bigg[(\Delta t)^2\int_0^T\left(\|\partial_{tt}\boldsymbol{u}\|^2_{H^1(\Omega)} + \|\partial_{tt}\xi\|^2_{L^2(\Omega)} + \|\partial_{tt}p\|^2_{L^2(\Omega)}\right)ds \\
&\quad + h^{2k}\int_0^T\left(\|\partial_t\boldsymbol{u}\|^2_{H^{k+1}(\Omega)} + \|\partial_t\xi\|^2_{H^k(\Omega)}\right)ds + h^{2l+2}\int_0^T\|\partial_t p\|^2_{H^{l+1}(\Omega)}ds\Bigg].
\end{aligned}$$

Here, the constant $\tilde{C}$ has the following estimate:

$$\tilde{C} = \tilde{C}(T, c_0, \lambda, \alpha) \lesssim exp(CT)\left(1 + c_0 + \frac{1+\alpha^2}{\lambda} + \frac{1+\alpha^2}{\lambda^2}\right).$$

Since the inequality $\|e_\xi^{N+1}\|^2_{L^2(\Omega)} \lesssim \mu\|\varepsilon(e_{\boldsymbol{u}}^{h,N+1})\|^2_{L^2(\Omega)}$ is implied in (62), we can use (63) to deduce the desired result (54). This completes the proof. □

Corollary 1 *Let* $(\boldsymbol{u}, \xi, p)$ *and* $(\boldsymbol{u}_h^{n+1}, \xi_h^{n+1}, p_h^{n+1})$ *for* $n \geq 1$ *be the solutions of Eqs.* (11)–(13) *and Eqs.* (28)–(30)*, respectively. Under* ***Assumption*** 1*, there holds*

$$\begin{aligned}
&\sqrt{\mu}\|\varepsilon(e_{\boldsymbol{u}}^{N+1})\|_{L^2(\Omega)} + \|e_\xi^{N+1}\|_{L^2(\Omega)} \\
&\quad + \sqrt{c_0 + \frac{\alpha^2}{\lambda}}\|e_p^{N+1}\|_{L^2(\Omega)} \lesssim (\Delta t + h^k + h^{l+1}),
\end{aligned} \tag{64}$$

$$\sqrt{K}\|\nabla e_p^{N+1}\|_{L^2(\Omega)} \lesssim (\Delta t + h^k + h^l). \tag{65}$$

Proof Applying the triangle inequality, we observe that the following inequality holds.

$$\begin{aligned}
&\sqrt{\mu}\|\varepsilon(e_{\boldsymbol{u}}^{N+1})\|_{L^2(\Omega)} + \|e_\xi^{N+1}\|_{L^2(\Omega)} + \sqrt{c_0 + \frac{\alpha^2}{\lambda}}\|e_p^{N+1}\|_{L^2(\Omega)} \\
&\le \underbrace{\left(\sqrt{\mu}\|\varepsilon(e_{\boldsymbol{u}}^{I,N+1})\|_{L^2(\Omega)} + \|e_\xi^{I,N+1}\|_{L^2(\Omega)} + \sqrt{c_0 + \frac{\alpha^2}{\lambda}}\|e_p^{I,N+1}\|_{L^2(\Omega)}\right)}_{\mathbf{I}} \\
&+ \underbrace{\left(\sqrt{\mu}\|\varepsilon(e_{\boldsymbol{u}}^{h,N+1})\|_{L^2(\Omega)} + \|e_\xi^{h,N+1}\|_{L^2(\Omega)} + \sqrt{c_0 + \frac{\alpha^2}{\lambda}}\|e_p^{h,N+1}\|_{L^2(\Omega)}\right)}_{\mathbf{II}}.
\end{aligned} \tag{66}$$

To estimate **I**, we apply the estimates for projection operators (19) and (21). There holds

$$\mathbf{I} \lesssim h^k(\|\boldsymbol{u}^{N+1}\|_{H^{k+1}(\Omega)} + \|\xi^{N+1}\|_{H^k(\Omega)}) + h^{l+1}\|p^{N+1}\|_{H^{l+1}(\Omega)}.$$

The bound of **II** can be estimated directly from inequality (54) in Theorem 3. Then, we see that (64) holds. Similarly, the following inequality holds true.

$$\sqrt{K}\|\nabla e_p^{N+1}\|_{L^2(\Omega)} \le \underbrace{\sqrt{K}\|\nabla e_p^{I,N+1}\|_{L^2(\Omega)}}_{\mathbf{III}} + \underbrace{\sqrt{K}\|\nabla e_p^{h,N+1}\|_{L^2(\Omega)}}_{\mathbf{IV}}. \tag{67}$$

The estimate for projection operator (20) provides $\mathbf{III} \lesssim h^l\|p^{N+1}\|_{H^{l+1}(\Omega)}$. The bound of **IV** can be estimated by inequality (38) in Theorem 2. Then we complete the proof of (65). □

4.2 A Priori Error Estimates for the RtS Algorithm

In this subsection, we give the a priori error estimates of the **RtS algorithm**. The main conclusions are similar to those in the previous subsection, but the proofs are slightly different.

Theorem 4 *Let* $(\boldsymbol{u}, \xi, p)$ *and* $(\boldsymbol{u}_h^{n+1}, \xi_h^{n+1}, p_h^{n+1})$ *for* $n \ge 1$ *be the solutions of Eqs.* (11)–(13) *and Eqs.* (31)–(33)*, respectively. Under* ***Assumption*** 1*, there holds*

$$\begin{aligned}
&\sum_{n=1}^{N}\left(\mu\|\varepsilon(D_{\boldsymbol{u}}^{n+1})\|_{L^2(\Omega)}^2 + \frac{1}{4\lambda}\|\alpha D_p^{n+1} - D_\xi^{n+1}\|_{L^2(\Omega)}^2\right) + \frac{K}{2}\Delta t\|\nabla e_p^{h,N+1}\|_{L^2(\Omega)}^2 \\
&\le \tilde{C}\Bigg[(\Delta t)^3\int_0^T\left(\|\partial_{tt}\boldsymbol{u}\|_{H^1(\Omega)}^2 + \|\partial_{tt}\xi\|_{L^2(\Omega)}^2 + \|\partial_{tt}p\|_{L^2(\Omega)}^2\right)ds \\
&+ h^{2k}\Delta t\int_0^T\left(\|\partial_t\boldsymbol{u}\|_{H^{k+1}(\Omega)}^2 + \|\partial_t\xi\|_{H^k(\Omega)}^2\right)ds + h^{2l+2}\Delta t\int_0^T\|\partial_t p\|_{H^{l+1}(\Omega)}^2 ds\Bigg].
\end{aligned} \tag{68}$$

Here, $\tilde{C} = \tilde{C}(c_0, \lambda, \alpha)$.

Proof We subtract (31), (32), (33) from (11), (12), (13), respectively, to derive

$$a_1(e_{\boldsymbol{u}}^{n+1}, \boldsymbol{v}_h) - b(\boldsymbol{v}_h, e_\xi^{n+1}) = 0,$$

$$b(e_{\boldsymbol{u}}^{n+1}-e_{\boldsymbol{u}}^{n},\phi_h)+a_2(e_{\xi}^{n+1}-e_{\xi}^{n},\phi_h)=c(e_p^{n+1}-e_p^{n},\phi_h),$$
$$a_3\left(\partial_t p^{n+1}-\frac{p_h^{n+1}-p_h^{n}}{\Delta t},\psi_h\right)+d(e_p^{n+1},\psi_h)=c\left(\psi_h,\partial_t\xi^{n+1}-\frac{\xi_h^{n}-\xi_h^{n-1}}{\Delta t}\right).$$

By using the projection operators (16), (17) and (18), one has

$$a_1(e_{\boldsymbol{u}}^{h,n+1},\boldsymbol{v}_h)-b(\boldsymbol{v}_h,e_{\xi}^{h,n+1})=0, \tag{69}$$
$$b(D_{\boldsymbol{u}}^{n+1},\phi_h)+a_2(e_{\xi}^{n+1}-e_{\xi}^{n},\phi_h)=c(e_p^{n+1}-e_p^{n},\phi_h), \tag{70}$$
$$\begin{aligned}&a_3(D_p^{n+1},\psi_h)-c(\psi_h,D_{\xi}^{n})+\Delta t d(e_p^{h,n+1},\psi_h)\\&=a_3(R_p p^{n+1}-R_p p^{n}-\Delta t\partial_t p^{n+1},\psi_h)-c(\psi_h,R_{\xi}\xi^{n}-R_{\xi}\xi^{n-1}-\Delta t\partial_t\xi^{n+1}).\end{aligned} \tag{71}$$

We apply the same technique as that used in (42) and (46) to derive

$$a_1(D_{\boldsymbol{u}}^{n+1},\boldsymbol{v}_h)-b(\boldsymbol{v}_h,D_{\xi}^{n+1})=0, \tag{72}$$
$$\begin{aligned}&b(D_{\boldsymbol{u}}^{n+1},\phi_h)+a_2(D_{\xi}^{n+1},\phi_h)-c(D_p^{n+1},\phi_h)=b(\boldsymbol{u}^{n+1}-\boldsymbol{u}^{n}-\Delta t\partial_t\boldsymbol{u}^{n+1},\phi_h)\\&\quad+a_2(R_{\xi}\xi^{n+1}-R_{\xi}\xi^{n}-\Delta t\partial_t\xi^{n+1},\phi_h)-c(R_p p^{n+1}-R_p p^{n}-\Delta t\partial_t p^{n+1},\phi_h).\end{aligned} \tag{73}$$

Again, we take $\boldsymbol{v}_h=D_{\boldsymbol{u}}^{n+1}$ in (72), $\phi_h=D_{\xi}^{n+1}$ in (73) and $\psi_h=D_p^{n+1}$ in (71) to obtain

$$\begin{aligned}&a_1(D_{\boldsymbol{u}}^{n+1},D_{\boldsymbol{u}}^{n+1})+a_2(D_{\xi}^{n+1},D_{\xi}^{n+1})+a_3(D_p^{n+1},D_p^{n+1})\\&\quad-c(D_p^{n+1},D_{\xi}^{n+1})+\Delta t d(e_p^{h,n+1},D_p^{n+1})\\&=b(\boldsymbol{u}^{n+1}-\boldsymbol{u}^{n}-\Delta t\partial_t\boldsymbol{u}^{n+1},D_{\xi}^{n+1})+a_2(R_{\xi}\xi^{n+1}-R_{\xi}\xi^{n}-\Delta t\partial_t\xi^{n+1},D_{\xi}^{n+1})\\&\quad+c(\Delta t\partial_t p^{n+1}-R_p p^{n+1}+R_p p^{n},D_{\xi}^{n+1})+a_3(R_p p^{n+1}-R_p p^{n}-\Delta t\partial_t p^{n+1},D_p^{n+1})\\&\quad+c(D_p^{n+1},\Delta t\partial_t\xi^{n+1}-R_{\xi}\xi^{n}+R_{\xi}\xi^{n-1})+c(D_p^{n+1},D_{\xi}^{n}).\end{aligned} \tag{74}$$

Applying (48) to the left hand side of (74), and taking the summation over the index n from 1 to N yields

$$\begin{aligned}&\sum_{n=1}^{N}\left[2\mu\|\varepsilon(D_{\boldsymbol{u}}^{n+1})\|_{L^2(\Omega)}^2+\frac{1}{2\lambda}\|D_{\xi}^{n+1}\|_{L^2(\Omega)}^2+\left(c_0+\frac{\alpha^2}{2\lambda}\right)\|D_p^{n+1}\|_{L^2(\Omega)}^2\right.\\&\quad\left.+\frac{1}{2\lambda}\|\alpha D_p^{n+1}-D_{\xi}^{n+1}\|_{L^2(\Omega)}^2\right]+\Delta t\sum_{n=1}^{N}d(e_p^{h,n+1},D_p^{n+1})=\sum_{i}^{6}\tilde{T}_i,\end{aligned} \tag{75}$$

where

$$\tilde{T}_1=T_1,\quad \tilde{T}_2=T_2,\quad \tilde{T}_3=\sum_{n=1}^{N}c(\Delta t\partial_t p^{n+1}-R_p p^{n+1}+R_p p^{n},D_{\xi}^{n+1}),$$
$$\tilde{T}_4=T_4,\quad \tilde{T}_5=\sum_{n=1}^{N}c(D_p^{n+1},\Delta t\partial_t\xi^{n+1}-R_{\xi}\xi^{n}+R_{\xi}\xi^{n-1}),\quad \tilde{T}_6=\sum_{n=1}^{N}c(D_p^{n+1},D_{\xi}^{n}).$$

Since $\tilde{T}_1,\tilde{T}_2,\tilde{T}_4$ are estimated in Theorem 2 already, here we estimate $\tilde{T}_3,\tilde{T}_5,\tilde{T}_6$ by using the Cauchy-Schwarz inequality, Young's inequality, (19), (21), and (36) with any $\epsilon_1>0$ and $\epsilon_2>0$.

$$\tilde{T}_3 \le \frac{\epsilon_1}{3}\sum_{n=1}^{N}\|D_\xi^{n+1}\|_{L^2(\Omega)}^2 + \frac{C\alpha^2}{\epsilon_1\lambda^2}\Big[(\Delta t)^3\int_0^T \|\partial_{tt}p\|_{L^2(\Omega)}^2 ds + h^{2l+2}\Delta t\int_0^T \|\partial_t p\|_{H^{l+1}(\Omega)}^2 ds\Big],$$

$$\tilde{T}_5 = \sum_{n=1}^{N}\Big[c(D_p^{n+1}, \Delta t\partial_t\xi^{n+1} - \Delta t\partial_t\xi^n) + c(D_p^{n+1}, \Delta t\partial_t\xi^n - R_\xi\xi^n + R_\xi\xi^{n-1})\Big]$$
$$\le \frac{\epsilon_2\alpha^2}{4}\sum_{n=1}^{N}\|D_p^{n+1}\|_{L^2(\Omega)}^2 + \frac{C}{\epsilon_2\lambda^2}\Big[(\Delta t)^3\int_0^T \|\partial_{tt}\xi\|_{L^2(\Omega)}^2 ds + h^{2k}\Delta t\int_0^T \left(\|\partial_t\boldsymbol{u}\|_{H^{k+1}(\Omega)}^2 + \|\partial_t\xi\|_{H^k(\Omega)}^2\right) ds\Big],$$

$$\tilde{T}_6 = \sum_{n=1}^{N}\frac{\alpha}{\lambda}\int_\Omega D_p^{n+1}D_\xi^n \le \frac{\alpha^2}{2\lambda}\sum_{n=1}^{N}\|D_p^{n+1}\|_{L^2(\Omega)}^2 + \frac{1}{2\lambda}\sum_{n=1}^{N}\|D_\xi^n\|_{L^2(\Omega)}^2.$$

Applying the bounds of $\tilde{T}_i$ for $i = 1, 2, \ldots, 6$ to (75), we see that

$$\sum_{n=1}^{N}\Big[2\mu\|\varepsilon(D_{\boldsymbol{u}}^{n+1})\|_{L^2(\Omega)}^2 + \frac{1}{2\lambda}\|D_\xi^{n+1}\|_{L^2(\Omega)}^2 + \frac{1}{2\lambda}\|\alpha D_p^{n+1} - D_\xi^{n+1}\|_{L^2(\Omega)}^2\Big]$$
$$+ \frac{K}{2}\Delta t\|\nabla e_p^{h,N+1}\|_{L^2(\Omega)}^2 - \frac{K}{2}\Delta t\|\nabla e_p^{h,1}\|_{L^2(\Omega)}^2$$
$$\le \epsilon_1\sum_{n=1}^{N}\|D_\xi^{n+1}\|_{L^2(\Omega)}^2 + \frac{\epsilon_2\alpha^2}{2}\sum_{n=1}^{N}\|D_p^{n+1}\|_{L^2(\Omega)}^2 + \frac{1}{2\lambda}\sum_{n=1}^{N}\|D_\xi^n\|_{L^2(\Omega)}^2$$
$$+ \tilde{C}\Big[(\Delta t)^3\int_0^T \left(\|\partial_{tt}\boldsymbol{u}\|_{H^1(\Omega)}^2 + \|\partial_{tt}\xi\|_{L^2(\Omega)}^2 + \|\partial_{tt}p\|_{L^2(\Omega)}^2\right) ds$$
$$+ h^{2k}\Delta t\int_0^T \left(\|\partial_t\boldsymbol{u}\|_{H^{k+1}(\Omega)}^2 + \|\partial_t\xi\|_{H^k(\Omega)}^2\right) ds + h^{2l+2}\Delta t\int_0^T \|\partial_t p\|_{H^{l+1}(\Omega)}^2 ds\Big].$$

Next, the same technique used in Theorem 2 is applied here, with a slight difference between the terms $\tilde{T}_6$ and T_6. Recalling that (52) and (53) hold true here, we can determine coefficients $\epsilon_1 = \frac{\tilde{\beta}}{4C_1}$ and $\epsilon_2 = \min\{\frac{1}{4\lambda}, \frac{\tilde{\beta}}{4C_1}\}$. Then, we apply (34) to handle the terms $\|D_\xi^1\|_{L^2(\Omega)}^2$, $\|\nabla e_p^{h,1}\|_{L^2(\Omega)}^2$, which completes the proof of (68). □

Theorem 5 *Let* $(\boldsymbol{u}, \xi, p)$ *and* $(\boldsymbol{u}_h^{n+1}, \xi_h^{n+1}, p_h^{n+1})$ *for* $n \ge 1$ *be the solutions of Eqs.* (11)–(13) *and Eqs.* (31)–(33)*, respectively. Under* ***Assumption*** 1*, there holds*

$$\mu\|\varepsilon(e_{\boldsymbol{u}}^{h,N+1})\|_{L^2(\Omega)}^2 + \|e_\xi^{h,N+1}\|_{L^2(\Omega)}^2 + \left(c_0 + \frac{\alpha^2}{\lambda}\right)\|e_p^{h,N+1}\|_{L^2(\Omega)}^2$$
$$+ K\Delta t\sum_{n=1}^{N}\|\nabla e_p^{h,n+1}\|_{L^2(\Omega)}^2$$
$$\le \tilde{C}\Big[(\Delta t)^2\int_0^T \left(\|\partial_{tt}\boldsymbol{u}\|_{H^1(\Omega)}^2 + \|\partial_{tt}\xi\|_{L^2(\Omega)}^2 + \|\partial_{tt}p\|_{L^2(\Omega)}^2\right) ds$$

$$+ h^{2k} \int_0^T \left(\|\partial_t \boldsymbol{u}\|^2_{H^{k+1}(\Omega)} + \|\partial_t \xi\|^2_{H^k(\Omega)} \right) ds + h^{2l+2} \int_0^T \|\partial_t p\|^2_{H^{l+1}(\Omega)} ds \Big]. \tag{76}$$

Here, $\tilde{C} = \tilde{C}(T, c_0, \lambda, \alpha)$.

Proof Choosing $\boldsymbol{v}_h = D_{\boldsymbol{u}}^{n+1}$ in (69), $\phi_h = e_\xi^{h,n+1}$ in (73) and $\psi_h = e_p^{h,n+1}$ in (71), we have

$$a_1(e_{\boldsymbol{u}}^{h,n+1}, D_{\boldsymbol{u}}^{n+1}) - b(D_{\boldsymbol{u}}^{n+1}, e_\xi^{h,n+1}) = 0, \tag{77}$$

$$\begin{aligned} &b(D_{\boldsymbol{u}}^{n+1}, e_\xi^{h,n+1}) + a_2(D_\xi^{n+1}, e_\xi^{h,n+1}) - c(D_p^{n+1}, e_\xi^{h,n+1}) \\ &\quad = b(\boldsymbol{u}^{n+1} - \boldsymbol{u}^n - \Delta t \partial_t \boldsymbol{u}^{n+1}, e_\xi^{h,n+1}) + a_2(R_\xi \xi^{n+1} - R_\xi \xi^n - \Delta t \partial_t \xi^{n+1}, e_\xi^{h,n+1}) \\ &\quad - c(R_p p^{n+1} - R_p p^n - \Delta t \partial_t p^{n+1}, e_\xi^{h,n+1}), \end{aligned} \tag{78}$$

$$\begin{aligned} &a_3(D_p^{n+1}, e_p^{h,n+1}) - c(e_p^{h,n+1}, D_\xi^{n+1}) + \Delta t d(e_p^{h,n+1}, e_p^{h,n+1}) \\ &\quad = a_3(R_p p^{n+1} - R_p p^n - \Delta t \partial_t p^{n+1}, e_p^{h,n+1}) \\ &\quad - c(e_p^{h,n+1}, R_\xi \xi^n - R_\xi \xi^{n-1} - \Delta t \partial_t \xi^{n+1}) - c(e_p^{h,n+1}, D_\xi^{n+1} - D_\xi^n). \end{aligned} \tag{79}$$

Similar to the previous proof, after summing up (77), (78), (79) over the index n from 1 to N, we can apply (37) and (59) to derive

$$\begin{aligned} &\frac{1}{2} \Big(2\mu \|\varepsilon(e_{\boldsymbol{u}}^{h,N+1})\|^2_{L^2(\Omega)} - 2\mu \|\varepsilon(e_{\boldsymbol{u}}^{h,1})\|^2_{L^2(\Omega)} + c_0 \|e_p^{h,N+1}\|^2_{L^2(\Omega)} \\ &\quad - c_0 \|e_p^{h,1}\|^2_{L^2(\Omega)} + \frac{1}{\lambda} \|\alpha e_p^{h,N+1} - e_\xi^{h,N+1}\|^2_{L^2(\Omega)} \\ &\quad - \frac{1}{\lambda} \|\alpha e_p^{h,1} - e_\xi^{h,1}\|^2_{L^2(\Omega)} \Big) + K \Delta t \sum_{n=1}^N \|\nabla e_p^{h,n+1}\|^2_{L^2(\Omega)} \le \sum_{i=1}^6 \tilde{E}_i, \end{aligned} \tag{80}$$

where

$$\tilde{E}_1 = E_1, \quad \tilde{E}_2 = E_2, \quad \tilde{E}_3 = \sum_{n=1}^N c(\Delta t \partial_t p^{n+1} - R_p p^{n+1} + R_p p^n, e_\xi^{h,n+1}),$$

$$\tilde{E}_4 = E_4, \quad \tilde{E}_5 = \sum_{n=1}^N c(e_p^{h,n+1}, \Delta t \partial_t \xi^{n+1} - R_\xi \xi^n + R_\xi \xi^{n-1}),$$

$$\tilde{E}_6 = \sum_{n=1}^N c(-e_p^{h,n+1}, D_\xi^{n+1} - D_\xi^n).$$

The bounds of $\tilde{E}_1, \tilde{E}_2, \tilde{E}_4$ have been estimated in Theorem 3. Using the Cauchy-Schwarz inequality, Young's inequality, the Poincaré inequality, (19), (21), and (36), we can estimate $\tilde{E}_3, \tilde{E}_5, \tilde{E}_6$ with any $\epsilon_1 > 0, \epsilon_2 > 0, \epsilon_3 > 0$ as follows.

$$\begin{aligned} \tilde{E}_3 &\le \frac{\epsilon_1}{6} \Delta t \sum_{n=1}^N \|e_\xi^{h,n+1}\|^2_{L^2(\Omega)} + \frac{C\alpha^2}{\epsilon_1 \lambda^2} \Big[(\Delta t)^2 \int_0^T \|\partial_{tt} p\|^2_{L^2(\Omega)} ds \\ &\quad + h^{2l+2} \int_0^T \|\partial_t p\|^2_{H^{l+1}(\Omega)} ds \Big]. \end{aligned}$$

$$\tilde{E}_5 = \sum_{n=1}^N \Big[c(e_p^{h,n+1}, \Delta t \partial_t \xi^{n+1} - \Delta t \partial_t \xi^n) + c(e_p^{h,n+1}, \Delta t \partial_t \xi^n - R_\xi \xi^n + R_\xi \xi^{n-1}) \Big]$$

$$\leq \frac{\epsilon_2\alpha^2}{8}\Delta t\sum_{n=1}^{N}\|e_p^{h,n+1}\|_{L^2(\Omega)}^2+\frac{C}{\epsilon_2\lambda^2}\Bigg[(\Delta t)^2\int_0^T\|\partial_{tt}\xi\|_{L^2(\Omega)}^2 ds$$
$$+h^{2k}\int_0^T\left(\|\partial_t\boldsymbol{u}\|_{H^{k+1}(\Omega)}^2+\|\partial_t\xi\|_{H^k(\Omega)}^2\right)ds\Bigg],$$
$$\tilde{E}_6=\sum_{n=1}^{N}\Big[-c(e_p^{h,n+1},D_\xi^{n+1})+c(D_p^{n+1},D_\xi^n)+c(e_p^{h,n},D_\xi^n)\Big]$$
$$=-c(e_p^{h,N+1},D_\xi^{N+1})+\sum_{n=1}^{N}c(D_p^{n+1},D_\xi^n)+c(e_p^{h,1},D_\xi^1)$$
$$\leq\sum_{n=1}^{N}\left(\frac{\alpha^2}{2\lambda}\|D_p^{n+1}\|_{L^2(\Omega)}^2+\frac{1}{2\lambda}\|D_\xi^{n+1}\|_{L^2(\Omega)}^2\right)+\frac{\epsilon_3\alpha^2}{2}\|e_p^{h,N+1}\|_{L^2(\Omega)}^2$$
$$+\frac{1}{\epsilon_3 2\lambda^2}\|D_\xi^{N+1}\|_{L^2(\Omega)}^2+\frac{\alpha^2}{2\lambda}\|e_p^{h,1}\|_{L^2(\Omega)}^2+\frac{1}{\lambda}\|D_\xi^1\|_{L^2(\Omega)}^2.$$

Using the bound of $\tilde{E}_i$ for $i=1,2,\ldots,6$, we can reformulate (80) to obtain

$$2\mu\|\varepsilon(e_{\boldsymbol{u}}^{h,N+1})\|_{L^2(\Omega)}^2-2\mu\|\varepsilon(e_{\boldsymbol{u}}^{h,1})\|_{L^2(\Omega)}^2+c_0\|e_p^{h,N+1}\|_{L^2(\Omega)}^2-c_0\|e_p^{h,1}\|_{L^2(\Omega)}^2$$
$$+\frac{1}{\lambda}\|\alpha e_p^{h,N+1}-e_\xi^{h,N+1}\|_{L^2(\Omega)}^2-\frac{1}{\lambda}\|\alpha e_p^{h,1}-e_\xi^{h,1}\|_{L^2(\Omega)}^2+2K\Delta t\sum_{n=1}^{N}\|\nabla e_p^{h,n+1}\|_{L^2(\Omega)}^2$$
$$\leq\epsilon_1\Delta t\sum_{n=1}^{N}\|e_\xi^{h,n+1}\|_{L^2(\Omega)}^2+c_0\Delta t\sum_{n=1}^{N}\|e_p^{h,n+1}\|_{L^2(\Omega)}^2+\frac{\epsilon_2\alpha^2}{2}\Delta t\sum_{n=1}^{N}\|e_p^{h,n+1}\|_{L^2(\Omega)}^2$$
$$+\epsilon_3\alpha^2\|e_p^{h,N+1}\|_{L^2(\Omega)}^2+\sum_{n=1}^{N}\frac{\alpha^2}{\lambda}\|D_p^{n+1}\|_{L^2(\Omega)}^2+\sum_{n=1}^{N}\frac{1}{\lambda}\|D_\xi^{n+1}\|_{L^2(\Omega)}^2+\frac{1}{\epsilon_3\lambda^2}\|D_\xi^{N+1}\|_{L^2(\Omega)}^2$$
$$+\tilde{C}\Bigg[(\Delta t)^2\int_0^T\left(\|\partial_{tt}\boldsymbol{u}\|_{H^1(\Omega)}^2+\|\partial_{tt}\xi\|_{L^2(\Omega)}^2+\|\partial_{tt}p\|_{L^2(\Omega)}^2\right)ds$$
$$+h^{2k}\int_0^T\left(\|\partial_t\boldsymbol{u}\|_{H^{k+1}(\Omega)}^2+\|\partial_t\xi\|_{H^k(\Omega)}^2\right)ds+h^{2l+2}\int_0^T\|\partial_t p\|_{H^{l+1}(\Omega)}^2 ds\Bigg]$$
$$+\frac{\alpha^2}{\lambda}\|e_p^{h,1}\|_{L^2(\Omega)}^2+\frac{2}{\lambda}\|D_\xi^1\|_{L^2(\Omega)}^2. \tag{81}$$

Next, the same technique used in Theorem 3 is applied here, with a slight difference between the terms $\tilde{E}_6$ and E_6. Recalling that (62) and (63) holds true here, we choose $\epsilon_1=\frac{\tilde{\beta}}{4C_1}$, $\epsilon_2=\min\{\frac{1}{2\lambda},\frac{\tilde{\beta}}{4C_1}\}$, $\epsilon_3=\min\{\frac{1}{2\lambda},\frac{\tilde{\beta}}{2C_1}\}$ to handle the first, third, fourth terms on the right-hand side. We can apply (68) to bound the summations of $\|D_\xi^{n+1}\|_{L^2(\Omega)}^2$, $\|D_p^{n+1}\|_{L^2(\Omega)}^2$, and use (35) to handle $\|e_p^{h,1}\|_{L^2(\Omega)}^2$, $\|D_\xi^1\|_{L^2(\Omega)}^2$. Finally, applying the discrete Grönwall's inequality, we come to the conclusion that the desired result (76) holds by using (62). □

Corollary 2 *Let* $(\boldsymbol{u},\xi,p)$ *and* $(\boldsymbol{u}_h^{n+1},\xi_h^{n+1},p_h^{n+1})$ *for* $n\geq 1$ *be the solutions to problems* (11)–(13) *and* (31)–(33)*, respectively. Under* ***Assumption*** 1*, there holds*

$$\sqrt{\mu}\|\varepsilon(e_{\boldsymbol{u}}^{N+1})\|_{L^2(\Omega)}+\|e_\xi^{N+1}\|_{L^2(\Omega)}$$

$$+\sqrt{c_0+\frac{\alpha^2}{\lambda}}\|e_p^{N+1}\|_{L^2(\Omega)} \lesssim \Delta t + h^k + h^{l+1}, \tag{82}$$

$$\sqrt{K}\|\nabla e_p^{N+1}\|_{L^2(\Omega)} \lesssim \Delta t + h^k + h^l. \tag{83}$$

Proof The same technique as that used in **Corollary** 1 is applied here. Firstly, (82) can be obtained from the projection estimates (19), (21), and (76) in Theorem 5. Applying the projection estimate (20) and (68) in Theorem 4, we see that (83) holds true. □

5 Benchmark Tests

In this section, we carry out numerical examples on two-dimensional domains to validate the theoretical predictions described in Sect. 4. Some benchmark tests that have been reported in the literature [14, 20, 33] are considered here. We will test the convergence rates under various settings of the time step size Δt, the mesh size h, finite element polynomial degrees k and l, and other physical parameters. All computations are implemented in the open-source software FEniCS [2].

Example 1 Let $\Omega = [0,1]^2$ and the final time is $T = 1.0$. We choose the body force $\boldsymbol{f}$, the source/sink term Q_s, initial conditions and Dirichlet boundary data on $\partial\Omega = \Gamma_{\boldsymbol{u}} = \Gamma_p$ such that the exact solution is as follows:

$$u_1 = \frac{1}{10}e^t(x+y^3), \quad u_2 = \frac{1}{10}t^2(x^3+y^3), \quad p = 10e^{\frac{x+y}{10}}(1+t^3).$$

Following [14], the other physical parameters are chosen as follows:

$$\mu = 1.0, \quad \lambda = 1.0, \quad c_0 = 1.0, \quad \alpha = 1.0, \quad K = 1.0.$$

To show the convergence orders in time, we fix the mesh size $h = \frac{1}{64}$, use $k = 3$, $l = 2$ in spatial discretization, and refine the time step size Δt. In Table 1, we summarize the results of errors and convergence orders in time. We observe that the orders of $\boldsymbol{H}^1$-error of $\boldsymbol{u}$, the L^2-error of ξ, and the L^2 & H^1 errors of p are all around 1, which verifies the theoretical analysis of the time error order.

Example 2 Let $\Omega = [0,1]^2$ with $\Gamma_1 = \{(1,y); 0 \le y \le 1\}$, $\Gamma_2 = \{(x,0); 0 \le x \le 1\}$, $\Gamma_3 = \{(0,y); 0 \le y \le 1\}$, $\Gamma_4 = \{(x,1); 0 \le x \le 1\}$ and the final time $T = 1.0$. Let Neumann boundary $\Gamma_N = \Gamma_2 \cup \Gamma_4 = \Gamma_\sigma \cup \Gamma_q$, and Dirichlet boundary $\Gamma_D = \Gamma_1 \cup \Gamma_3 = \Gamma_{\boldsymbol{u}} \cup \Gamma_p$. We choose the body force $\boldsymbol{f}$, the source/sink term Q_s, and initial conditions such that the exact solution is as follows:

$$u_1 = e^{-t}\left(\sin(2\pi y)(\cos(2\pi x)-1) + \frac{1}{\mu+\lambda}\sin(\pi x)\sin(\pi y)\right),$$

$$u_2 = e^{-t}\left(\sin(2\pi x)(1-\cos(2\pi y)) + \frac{1}{\mu+\lambda}\sin(\pi x)\sin(\pi y)\right),$$

$$p = e^{-t}\sin(\pi x)\sin(\pi y).$$

The fixed physical parameters are $E = 1.0$, $\alpha = 1.0$. To verify the theoretical error estimates, we consider the time step size and the mesh size to satisfy $\Delta t = (2h)^k = (2h)^{l+1}$.

First, we consider parameters $\nu = 0.3$, $K = 1.0$, $c_0 = 1.0$. In Table 2. We show the numerical convergence under the finite element discretization with the order $k = 2$ and

Table 1 Errors and convergence rates of different algorithms for Example 1

Method	Δt	$\boldsymbol{H}^1$-err of $\boldsymbol{u}$	Orders	L^2-err of ξ	Orders	L^2 & H^1 errs of p	Orders
StR alg.	1/4	9.276e−02		6.473e+00		1.769e−01 & 8.272e−01	
	1/8	5.536e−02	0.74	3.742e+00	0.79	1.250e−01 & 5.835e−01	0.50 & 0.50
	1/16	3.021e−02	0.87	2.005e+00	0.90	7.139e−02 & 3.331e−01	0.81 & 0.81
	1/32	1.577e−02	0.94	1.037e+00	0.95	3.792e−02 & 1.769e−01	0.91 & 0.91
	1/64	8.055e−03	0.97	5.271e−01	0.98	1.952e−02 & 9.104e−02	0.96 & 0.96
RtS alg.	1/4	3.907e−02		3.728e−01		1.753e−01 & 8.192e−01	
	1/8	2.332e−02	0.74	1.438e−01	1.37	1.228e−01 & 5.733e−01	0.51 & 0.51
	1/16	1.269e−02	0.88	6.964e−02	1.04	7.030e−02 & 3.280e−01	0.81 & 0.81
	1/32	6.625e−03	0.94	3.532e−02	0.98	3.736e−02 & 1.743e−01	0.91 & 0.91
	1/64	3.391e−03	0.97	1.794e−02	0.98	1.924e−02 & 8.973e−02	0.96 & 0.96

$l = 1$. From Table 2, we see that the orders of $\boldsymbol{H}^1$-error of $\boldsymbol{u}$, the L^2-error of ξ and the L^2-error of p are around 2, the order of H^1-error of p is around 1. While in Table 3, we summarize the results based on $k = 3$ and $l = 2$. From Table 3, we see that the orders of $\boldsymbol{H}^1$-error of $\boldsymbol{u}$, the L^2-error of ξ and the L^2-error of p are around 3, the order of H^1-error of p is around 2. From these two tables, our algorithms exhibit the optimal approximation orders.

Second, we consider parameters $\nu = 0.49999$ (correspondingly, $\lambda \approx 1.67 \times 10^5$), $K = 10^{-6}$, $c_0 = 0.0$ to test the robustness of the proposed schemes with respect to physical parameters. Some relevant tests of the robustness with respect to the material parameters can be founded in [20]. The numerical results for errors and convergence orders using the finite element order $k = 2$ and $l = 1$ are presented in Table 4. From the table, we can see that the proposed two algorithms also exhibit optimal order of convergence. The results indicate that our schemes are robust when λ is large and when K and/or c_0 are relatively small.

Example 3 We consider the point-source benchmark in poroelasticity called the Barry-Mercer's problem [4, 19, 28, 29], for which an analytical series solution is available. We assume that the width and length of the domain Ω satisfy $a = b = 1$. The boundary: $\Gamma_1 = \{(1, y); 0 \le y \le 1\}$, $\Gamma_2 = \{(x, 0); 0 \le x \le 1\}$, $\Gamma_3 = \{(0, y); 0 \le y \le 1\}$, $\Gamma_4 = \{(x, 1); 0 \le x \le 1\}$. The source/sink term Q_s is located at the point $(x_0, y_0) = (0.25, 0.25)$. The description of the boundary conditions and problem setting is shown in Fig. 2. The initial and boundary conditions are given as follows.

$$\begin{aligned} \boldsymbol{u} = 0,\ p = 0 \quad & \text{in } \Omega \times \{0\}, \\ u_1 = 0 \quad & \text{on } \Gamma_j \times (0, T],\ j = 2, 4, \\ u_2 = 0 \quad & \text{on } \Gamma_j \times (0, T],\ j = 1, 3, \\ p = 0,\ \boldsymbol{h} = \boldsymbol{0},\ g_2 = 0 \quad & \text{on } \Gamma_j \times (0, T],\ j = 1, 2, 3, 4. \end{aligned}$$

The body force term $\boldsymbol{f} = \boldsymbol{0}$, and the source/sink term

$$Q_s = 2\beta\delta(x - x_0)\delta(y - y_0)\sin(\beta t),$$

where $\beta = (\lambda + 2\mu)K$, $\delta(\cdot)$ represents the Dirac function. The physical parameters are given as:

$$c_0 = 0.0, \quad \alpha = 1.0, \quad E = 10^5, \quad \nu = 0.1, \quad K = 10^{-2}.$$

Denote $\lambda_n = n\pi$, $\lambda_q = q\pi$, and $\lambda_{nq} = \lambda_n^2 + \lambda_q^2$, then the analytical solution is as follows:

$$\begin{aligned} p(x, y, t) &= -4(\lambda + 2\mu) \sum_{n=1}^{\infty} \sum_{q=1}^{\infty} \hat{p}(n, q, t) \sin(\lambda_n x) \sin(\lambda_q y), \\ u_1(x, y, t) &= 4 \sum_{n=1}^{\infty} \sum_{q=1}^{\infty} \hat{u}_1(n, q, t) \cos(\lambda_n x) \sin(\lambda_q y), \\ u_2(x, y, t) &= 4 \sum_{n=1}^{\infty} \sum_{q=1}^{\infty} \hat{u}_2(n, q, t) \sin(\lambda_n x) \cos(\lambda_q y), \end{aligned}$$

where

$$\hat{p}(n, q, t) = -\frac{2 \sin(\lambda_n x_0) \sin(\lambda_q y_0)}{\lambda_{nq}^2 + 1} \left(\lambda_{nq} \sin(\beta t) - \cos(\beta t) + e^{-\lambda_{nq}\beta t}\right),$$

Table 2 Errors and convergence rates of different algorithms for Example 2 using FE orders $k = 2$ and $l = 1$ with $\nu = 0.3$, $K = 1.0$, $c_0 = 1.0$

Method	h	Δt	$\boldsymbol{H}^1$-err of $\boldsymbol{u}$	Orders	L^2-err of ξ	Orders	L^2& H^1 errs of p	Orders
StR alg.	1/4	1/4	5.600e−01		1.250e−01		2.597e−02 & 3.052e−01	
	1/8	1/16	1.516e−01	1.89	3.080e−02	2.02	6.724e−03 & 1.582e−01	1.95 & 0.95
	1/16	1/64	3.897e−02	1.96	7.749e−03	1.99	1.726e−03 & 7.994e−02	1.96 & 0.98
	1/32	1/256	9.823e−03	1.99	1.941e−03	2.00	4.346e−04 & 4.008e−02	1.99 & 1.00
RtS alg.	1/4	1/4	5.723e−01		1.463e−01		3.477e−02 & 3.285e−01	
	1/8	1/16	1.590e−01	1.85	4.448e−02	1.72	7.825e−03 & 1.590e−01	2.15 & 1.05
	1/16	1/64	4.213e−02	1.92	1.321e−02	1.75	1.995e−03 & 8.004e−02	1.97 & 0.99
	1/32	1/256	1.081e−02	1.96	3.607e−03	1.87	5.015e−04 & 4.009e−02	1.99 & 1.00

Table 3 Errors and convergence rates of different algorithms for Example 2 using FE orders $k = 3$ and $l = 2$ with $\nu = 0.3$, $K = 1.0$, $c_0 = 1.0$

Method	h	Δt	$\boldsymbol{H}^1$-err of $\boldsymbol{u}$	Orders	L^2-err of ξ	Orders	L^2& H^1 errs of p	Orders
StR alg.	1/4	1/8	1.426e−01		1.988e−02		3.136e−03 & 4.704e−02	
	1/8	1/64	1.598e−02	3.16	2.312e−03	3.10	3.919e−04 & 1.210e−02	3.00 & 1.96
	1/16	1/512	1.866e−03	3.10	2.632e−04	3.14	4.881e−05 & 3.068e−03	3.01 & 1.98
	1/32	1/4096	2.273e−04	3.04	3.102e−05	3.08	6.110e−06 & 7.721e−04	3.00 & 1.99
RtS alg.	1/4	1/8	1.546e−01		3.799e−02		8.361e−03 & 5.907e−02	
	1/8	1/64	1.769e−02	3.13	5.145e−03	2.88	9.495e−04 & 1.276e−02	3.14 & 2.21
	1/16	1/512	2.064e−03	3.10	6.300e−04	3.03	1.176e−04 & 3.109e−03	3.01 & 2.04
	1/32	1/4096	2.500e−04	3.05	7.705e−05	3.03	1.468e−05 & 7.746e−04	3.00 & 2.00

Table 4 Errors and convergence rates of different algorithms for Example 2 using FE orders $k = 2$ and $l = 1$ with $\nu = 0.49999$, $K = 10^{-6}$, $c_0 = 0.0$

Method	h	Δt	$\boldsymbol{H}^1$-err of $\boldsymbol{u}$	Orders	L^2-err of ξ	Orders	L^2& H^1 errs of p	Orders
StR alg.	1/4	1/4	5.343e−01		8.976e−02		9.539e−02 & 5.476e−01	
	1/8	1/16	1.445e−01	1.89	1.609e−02	2.48	2.182e−02 & 1.850e−01	2.13 & 1.57
	1/16	1/64	3.711e−02	1.96	3.659e−03	2.14	5.293e−03 & 8.332e−02	2.04 & 1.15
	1/32	1/256	9.355e−03	1.99	8.977e−04	2.03	1.308e−03 & 4.050e−02	2.02 & 1.04
RtS alg.	1/4	1/4	5.343e−01		8.976e−02		8.420e−02 & 5.797e−01	
	1/8	1/16	1.445e−01	1.89	1.609e−02	2.48	1.732e−02 & 1.933e−01	2.28 & 1.58
	1/16	1/64	3.711e−02	1.96	3.659e−03	2.14	4.200e−03 & 8.515e−02	2.04 & 1.18
	1/32	1/256	9.355e−03	1.99	8.977e−04	2.03	1.041e−03 & 4.076e−02	2.01 & 1.06

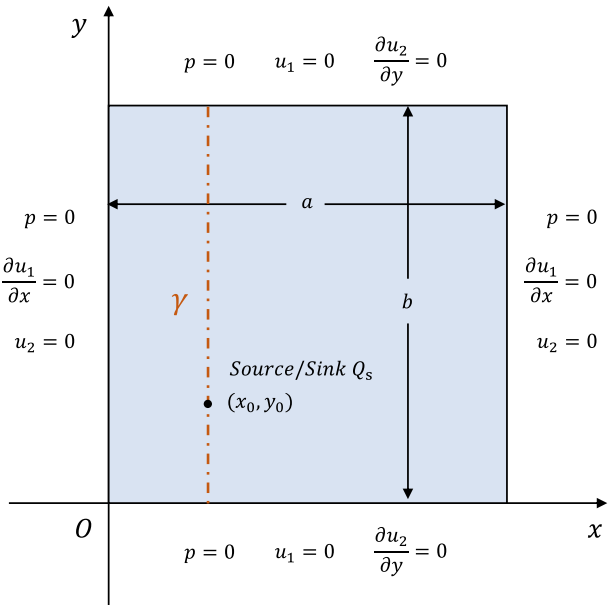

Fig. 2 Boundary conditions for the Barry-Mercer's problem

$$\hat{u}_1(n,q,t) = \frac{\lambda_n}{\lambda_{nq}}\hat{p}(n,q,t), \quad \hat{u}_2(n,q,t) = \frac{\lambda_q}{\lambda_{nq}}\hat{p}(n,q,t).$$

We conducted simulations for the Barry-Mercer's problem using the **Coupled algorithm**, the **StR algorithm**, and the **RtS algorithm** with finite element orders $k = 2$ and $l = 1$. The final time is set to $T = \pi/(2\beta)$, and a mesh size of $h = 1/64$ is used. Two different time step sizes, $\Delta t = \pi/(20\beta)$ and $\Delta t = \pi/(200\beta)$, are considered. The results of these simulations are presented in Fig. 3.

As shown in Fig. 3, we present the analytical solution and the numerical solutions obtained by using the different algorithms along a specified straight line $\gamma : x = 0.25$. From the results, the numerical solutions generated by the different approaches exhibit close agreement, particularly when employing a small time step size. The **RtS algorithm** and the **StR algorithm** exhibit stability and result in reliable solutions even with larger time step sizes, although their performance is slightly inferior to that of the **Coupled algorithm**.

Next, we conduct simulations to investigate the phenomenon of pressure oscillations by using a small permeability value of $K = 10^{-6}$ and a small time step size of $\Delta t = (\pi/2) \times 10^{-9}$. We recall that the proposed decoupled algorithms rely on the solutions computed by the **Coupled algorithm** for the first step. Different choices of finite element orders are considered in this experiment, and the results are presented in Fig. 4.

In the first step, we applied the **Coupled algorithm** and used subfigures **a**, **b**, and **c** to represent the results obtained with the $P_1 - P_1 - P_1$ method, $P_2 - P_1 - P_1$ method, and $P_3 - P_2 - P_2$ method, respectively. It is observed that the $P_1 - P_1 - P_1$ method exhibits pressure oscillations, while the $P_2 - P_1 - P_1$ method significantly reduces these oscillations, and the $P_3 - P_2 - P_2$ method performs the best by effectively eliminating pressure oscillations. Additionally, subfigure **d** displays the cross-section of the pressure at the line $\gamma : x = 0.25$ in the second time step using different algorithms with the $P_3 - P_2 - P_2$ method. Notably, no pressure oscillations were observed in this case. Furthermore, in comparison to the **RtS**

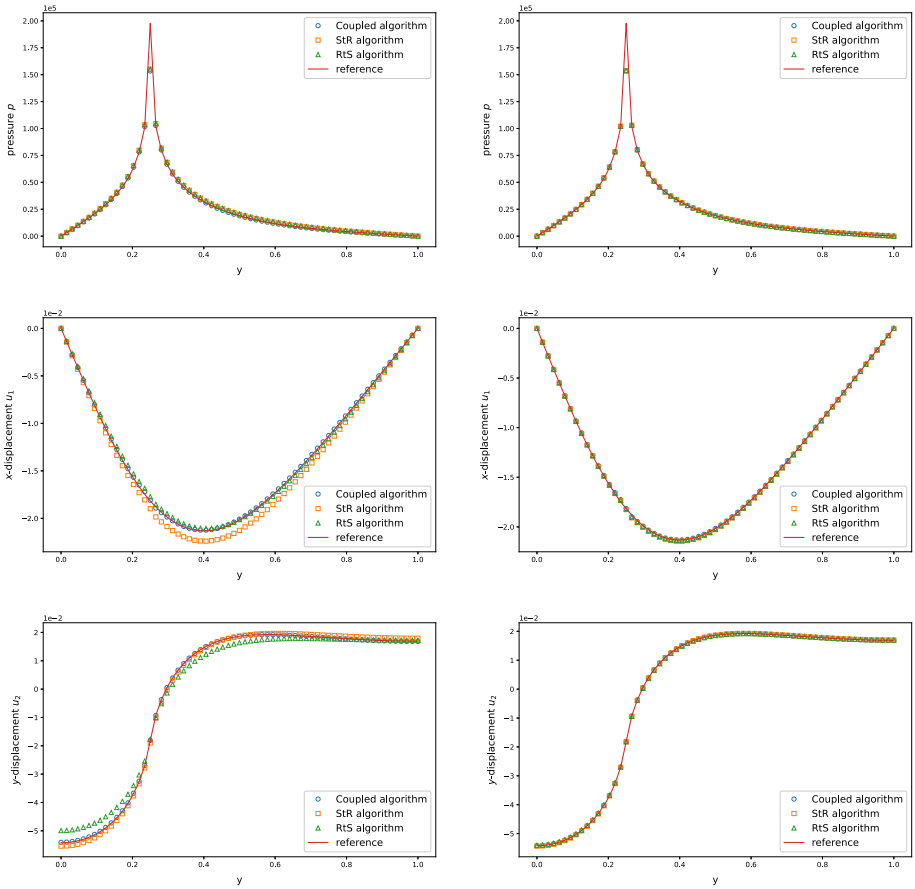

Fig. 3 The analytical solution, and the numerical solutions of the different algorithms for the pressure and the displacement along the line $\gamma\ x = 0.25$ at $T = \pi/(2\beta)$ with time step sizes $\Delta t = \pi/(20\beta)$ (left) and $\Delta t = \pi/(200\beta)$ (right)

algorithm, the **StR algorithm** demonstrates a performance that is more closely aligned with that of the **Coupled algorithm**.

6 Conclusions

In this paper, based on a new three-field formulation, we present some algorithms for decoupling the computation of Biot's model. A new theoretical framework is developed to analyze the algorithms. These algorithms only solve the system in a coupled way at the first time step. In the subsequent time steps, numerical computations are divided into solving two typical mathematical models. Error analysis is given to show that these algorithms are unconditionally stable and optimally convergent. Furthermore, numerical experiments are carried out to verify the prediction of error estimates. We highlight that our algorithms are unconditionally stable, efficient, and convergent in optimal order.

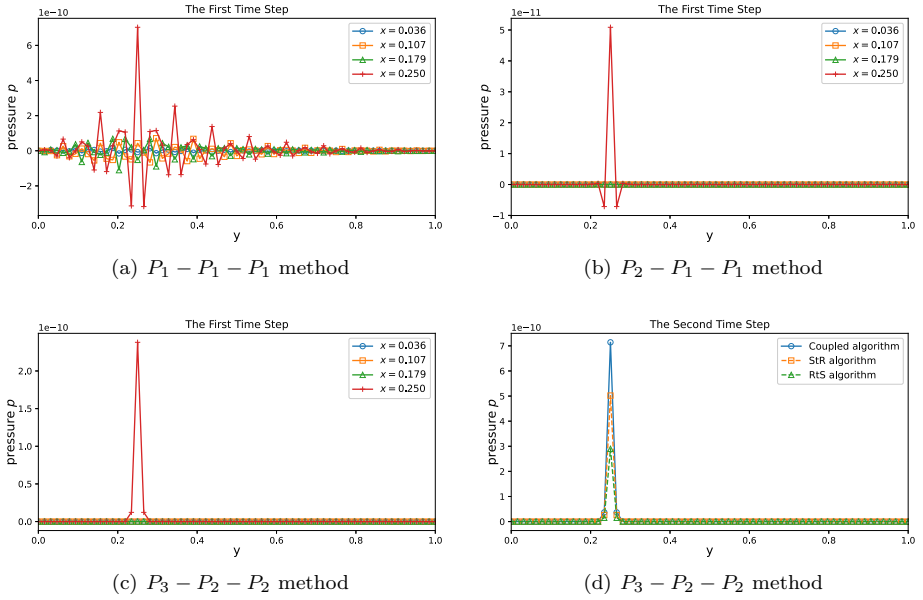

(a) $P_1 - P_1 - P_1$ method (b) $P_2 - P_1 - P_1$ method

(c) $P_3 - P_2 - P_2$ method (d) $P_3 - P_2 - P_2$ method

Fig. 4 Cross-sectional views of the pressure distribution for Barry-Mercer's problem. **a** Pressure cross-section using the $P_1 - P_1 - P_1$ method in the first step. **b** Pressure cross-section using the $P_2 - P_1 - P_1$ method in the first step. **c** Pressure cross-section using the $P_3 - P_2 - P_2$ method in the first step. (d) Cross-section of the pressure along the line $\gamma\ x = 0.25$ in the second time step, obtained using different algorithms with the $P_3 - P_2 - P_2$ method

Acknowledgements The work of M. Cai is partially supported by the NIH BUILD Grant through UL1GM118973, NIH-RCMI Grant through U54MD013376, XSEDE HPC allocation resource TG-MCH200-022, the Army Research Office award W911NF2310004, and the National Science Foundation awards (1700328, 1831950). The work of H. Gu and J. Li is partially supported by the NSF of China No. 11971221, Guangdong NSF Major Fund No. 2021ZDZX1001, the Shenzhen Sci-Tech Fund No. RCJC20200714114556020, JCYJ20200109115422828, and JCYJ20190809150413261, National Center for Applied Mathematics Shenzhen, and SUSTech International Center for Mathematics. The work of M. Mu is supported in part by the HongKong RGC CERG HKUST16301218.

Data Availability The FEniCS code and the datasets generated during and/or analyzed during the current study are shared in the following link https://github.com/cmchao2005/Decoupled-Algs-for-Biot.

Declarations

Conflict of interest The authors declare that they have no conflict of interest.

Human and Animal Rights This research does not involve human participants or animals.

References

1. Adler, J.H., Gaspar, F.J., Hu, X., Rodrigo, C., Zikatanov, L.T.: Robust block preconditioners for Biot's model. In: International Conference on Domain Decomposition Methods, pp. 3–16. Springer (2017)
2. Alnæs, M., Blechta, J., Hake, J., Johansson, A., Kehlet, B., Logg, A., Richardson, C., Ring, J., Rognes, M.E., Wells, G.N.: The FEniCS project version 1.5. Arch. Numer. Softw. **3**(100), 9–23 (2015)

3. Altmann, R., Maier, R., Unger, B.: Semi-explicit discretization schemes for weakly coupled elliptic-parabolic problems. Math. Comput. **90**(329), 1089–1118 (2021)
4. Barry, S., Mercer, G.: Exact solutions for two-dimensional time-dependent flow and deformation within a poroelastic medium. J. Appl. Mech. **66**(2), 536–540 (1999)
5. Biot, M.A.: General theory of three-dimensional consolidation. J. Appl. Phys. **12**(2), 155–164 (1941)
6. Biot, M.A.: Theory of elasticity and consolidation for a porous anisotropic solid. J. Appl. Phys. **26**(2), 182–185 (1955)
7. Both, J.W., Borregales, M., Nordbotten, J.M., Kumar, K., Radu, F.A.: Robust fixed stress splitting for Biot's equations in heterogeneous media. Appl. Math. Lett. **68**, 101–108 (2017)
8. Brenner, S.: A nonconforming mixed multigrid method for the pure displacement problem in planar linear elasticity. SIAM J. Numer. Anal. **30**(1), 116–135 (1993)
9. Brenner, S.C., Scott, L.R.: The Mathematical Theory of Finite Element Methods, vol. 3. Springer, Berlin (2008)
10. Bürger, R., Kumar, S., Mora, D., Ruiz-Baier, R., Verma, N.: Virtual element methods for the three-field formulation of time-dependent linear poroelasticity. Adv. Comput. Math. **47**(1), 1–37 (2021)
11. Cai, M., Ju, G., Li, J.: Schur complement based preconditioners for twofold and block tridiagonal saddle point problems. arXiv preprint arXiv:2108.08332 (2021)
12. Cai, M., Mu, M., Zhang, L.: Decoupling Techniques for Coupled PDE Models in Fluid Dynamics. IntechOpen, Berlin (2022)
13. Cai, M., Zhang, G.: Comparisons of some iterative algorithms for Biot equations. Int. J. Evol. Equ. **10**(3–4), 267–282 (2017)
14. Chaabane, N., Rivière, B.: A splitting-based finite element method for the Biot poroelasticity system. Comput. Math. Appl. **75**(7), 2328–2337 (2018)
15. Feng, X., Ge, Z., Li, Y.: Analysis of a multiphysics finite element method for a poroelasticity model. IMA J. Numer. Anal. **38**(1), 330–359 (2018)
16. Girault, V., Kumar, K., Wheeler, M.F.: Convergence of iterative coupling of geomechanics with flow in a fractured poroelastic medium. Comput. Geosci. **20**(5), 997–1011 (2016)
17. Gu, H., Cai, M., Li, J.: An iterative decoupled algorithm with unconditional stability for Biot model. Math. Comput. **92**(341), 1087–1108 (2023)
18. Gu, H., Cai, M., Li, J., Ju, G.: A priori error estimates of two monolithic schemes for Biot's consolidation model. Numerical Methods for Partial Differential Equations (2023)
19. Haghighat, E., Amini, D., Juanes, R.: Physics-informed neural network simulation of multiphase poroelasticity using stress-split sequential training. Comput. Methods Appl. Mech. Eng. **397**, 115141 (2022)
20. Ju, G., Cai, M., Li, J., Tian, J.: Parameter-robust multiphysics algorithms for Biot model with application in brain edema simulation. Math. Comput. Simul. **177**, 385–403 (2020)
21. Kim, J., Tchelepi, H.A., Juanes, R.: Stability and convergence of sequential methods for coupled flow and geomechanics: Fixed-stress and fixed-strain splits. Comput. Methods Appl. Mech. Eng. **200**(13–16), 1591–1606 (2011)
22. Lee, J.J.: Unconditionally stable second order convergent partitioned methods for multiple-network poroelasticity. arXiv preprint arXiv:1901.06078 (2019)
23. Lee, J.J., Mardal, K.A., Winther, R.: Parameter-robust discretization and preconditioning of Biot's consolidation model. SIAM J. Sci. Comput. **39**(1), A1–A24 (2017)
24. Lee, J.J., Piersanti, E., Mardal, K.A., Rognes, M.E.: A mixed finite element method for nearly incompressible multiple-network poroelasticity. SIAM J. Sci. Comput. **41**(2), A722–A747 (2019)
25. Mikelić, A., Wheeler, M.F.: Convergence of iterative coupling for coupled flow and geomechanics. Comput. Geosci. **17**(3), 455–461 (2013)
26. Nitsche, J.A.: On Korn's second inequality. RAIRO. Analyse Numérique **15**(3), 237–248 (1981)
27. Oyarzúa, R., Ruiz-Baier, R.: Locking-free finite element methods for poroelasticity. SIAM J. Numer. Anal. **54**(5), 2951–2973 (2016)
28. Phillips, P.J.: Finite Element Methods in Linear Poroelasticity: Theoretical and Computational Results. The University of Texas at Austin, Austin (2005)
29. Phillips, P.J., Wheeler, M.F.: Overcoming the problem of locking in linear elasticity and poroelasticity: an heuristic approach. Comput. Geosci. **13**(1), 5–12 (2009)
30. Qi, W., Seshaiyer, P., Wang, J.: Finite element method with the total stress variable for Biot's consolidation model. Numer. Methods Partial Differ. Equ. **37**(3), 2409–2428 (2021)
31. Rodrigo, C., Gaspar, F., Hu, X., Zikatanov, L.: Stability and monotonicity for some discretizations of the Biot's consolidation model. Comput. Methods Appl. Mech. Eng. **298**, 183–204 (2016)
32. Rodrigo, C., Hu, X., Ohm, P., Adler, J.H., Gaspar, F.J., Zikatanov, L.: New stabilized discretizations for poroelasticity and the Stokes' equations. Comput. Methods Appl. Mech. Eng. **341**, 467–484 (2018)

33. Yi, S.Y.: A study of two modes of locking in poroelasticity. SIAM J. Numer. Anal. **55**(4), 1915–1936 (2017)
34. Yi, S.Y., Bean, M.L.: Iteratively coupled solution strategies for a four-field mixed finite element method for poroelasticity. Int. J. Numer. Anal. Methods Geomech. **41**(2), 159–179 (2017)
35. Zhang, L., Cai, M., Mu, M.: Decoupling pde computation with intrinsic or inertial robin interface condition. Electron. Res. Arch. **29**(2), 2007–2028 (2021)

Authors and Affiliations

Mingchao Cai[1] · Huipeng Gu[2] · Jingzhi Li[3] · Mo Mu[4]

Huipeng Gu
12131226@mail.sustech.edu.cn

Jingzhi Li
li.jz@sustech.edu.cn

Mo Mu
mamu@ust.hk

1 Department of Mathematics, Morgan State University, 1700 East Cold Spring Lane, Baltimore, MD 21251, USA

2 Department of Mathematics, Southern University of Science and Technology, 1088 Nanshan District Xueyuan Road, Shenzhen 518055, Guangdong, China

3 Department of Mathematics & National Center for Applied Mathematics Shenzhen & SUSTech International Center for Mathematics, Southern University of Science and Technology, Shenzhen 518055, Guangdong, China

4 Department of Mathematics, Hong Kong University of Science and Technology, Clear Water Bay, Kowloon, Hong Kong